

Responses to Reviewer Comments on

Interactive comment on “Transport of regional pollutants through a remote trans-Himalayan valley in Nepal” by Shradda Dhungel et al.

We thank the two anonymous reviewers for their helpful comments on and recommendations for improvement of the subject manuscript. We have made major edits to the submitted version, which has helped improve the clarity of our presentation. The responses to Referee #1 and #2 are included in this document. Each comment is listed below followed by our response to that comment (in italics).

Referee #1

Received and published: 6 December 2016

GENERAL COMMENTS

This paper by Dhungel et al., 2016, provides a first characterization of the variability of ozone and equivalent BC at a measurement site located in a Himalayan valley. Until now only sparse continuous measurements are available in the Himalayas region. Thus the data presented in this work can be considered of high interest for the advancement of knowledge about SLCF (short-lived climate forcers) variability in the Himalaya and about the emissions and atmospheric processes able to affect them. Unfortunately, it is not clear from the paper, which data coverage is available over the whole (2.5-year long) investigation period.

However, the paper suffers of major deficiencies that prevent publication in this current form. Indeed, the paper only provides a basic characterization of typical seasonal and diurnal variability of O₃ and BC: only a tentative attribution of the observed variability in terms of valley wind regime. No information about the role of synoptic-scale transport variability is provided. The data analysis is basic and lacking of statistical analysis. The possible impact of open fire emissions in the IGP and Himalaya foothills should be better assessed by carrying out a systematic analysis. At least, the three case studies presented in Figure 6 should be better explored (as an instance by investigating them by using air-mass transport modeling and a better use of satellite data) and extended (e.g. no information is provided about the frequency by which the three “regimes” were observed over the whole measurement period). The occurrence of open fires is a typical feature of the pre-monsoon season in the Himalaya foothills. Why the transport of fire emission along the valley is observed only in a few cases? Which are the factors triggering the transport of open fire emissions?

Some previous works already extensively investigated the role of thermal wind circulation and open fire emission in affecting atmospheric composition in Himalaya (e.g. Bonasoni et al., ACP, 2010; Dumka et al., ACP, 2015; Lüthi et al., ACP, 2015; Xu et al., ACP, 2015; Raatikainen et al., Atmos. Env. 2014; Hyvärinen, ACP, 2011a,b). It should be great if the authors can discuss

their results as a function of these previous investigations even clarifying the scientific advance of their study in respect to these previous works. As an instance, the diurnal behaviors of BC and O₃ are significantly different from those observed at other Himalayan site (e.g. NCO-P, or Naintal ,see Bonasoni et al., 2010; Dumka et al., ACP, 2015) which reports eqBC increase from early morning and peaking in the afternoon. The authors should better motivate these differences. Finally, as also admitted by the authors, a not negligible influence on the observed behaviors could relate to local emissions (see the BC peak observed in the morning). It should be important (and interesting) that this local contribution is isolated and quantified before discussing eqBc and O₃ variability.

Moreover, I cannot able to find along the paper a real proof about the transport of pollution from IGP to TP: the paper only presents observations inside the Himalaya valley, thus the export of this pollution to TP is just a speculation at this stage. . .

Finally, I strongly suggest a language revision by a native-speaking English person.

In response to the reviewer's comment, we have: 1) added additional references to relevant previously published work; 2) added qualifications regarding interpretation of pollutant transport from the IGP; 3) statistically evaluated differences between the daytime and nighttime concentrations across seasons; 4) added seasonal flux patterns and calculated the net daily fluxes between different seasons with statistical analysis; 5)clarified characterization of the different types of transport episodes 6)added HYSPLIT back trajectories to the examples of transport episode.

SPECIFIC COMMENTS

Page 3, line 101. Extensive investigation of the role of valley wind system in favoring the transport of SLCFs to Himalayas was presented by Bonasoni et al., 2010 and reference therein. These researches can be profitably cited at this point of Introduction other than reporting the (rather dated) works from Alpine region. Also this work can be profitably cited: Quantification of topographic venting of boundary layer air to the free troposphere. S. Henne, M. Furger, S. Nyeki, M. Steinbacher, B. Neininger, S. F. J. de Wekker, J. Dommen, N. Spichtinger, A. Stohl, and A. S. H. Prévôt. Atmos. Chem. Phys., 4, 497-509, doi:10.5194/acp-4-497-2004, 2004.

The references section has been revised as follows:

“In the European Alps, prevailing wind systems in the mountain river valleys funnel polluted air from peripheral source regions to high elevations in a phenomenon known as “Alpine Pumping” (Weissmann et al., 2005). Under fair weather conditions during daytime, the upslope winds are capable of transporting significant pollutants and moisture into the free troposphere (Henne et al., 2004). Relative to air over plains, the

air within the valleys heats and cools more quickly (Steinacker, 1984). The resultant differences in temperature create gradients in pressure and density, which in turn drive transport of air from the plains to higher-elevations during the daytime (Reiter and Tang 1984, Whiteman and Bian, 1998; Egger et al., 2000). Numerous studies have looked at the possibility of the transport of pollutants from the IGP to the Himalayan foothills (Pant et al., 2006; Dumka et al., 2008; Komppula et al., 2009; Hyvärinen et al., 2009; Ram et al., 2010; Brun et al., 2011; Gautam et al., 2011; Srivastava et al., 2012). Other studies show that pollutants have the potential to reach not only the foothills of the Himalaya but also higher elevations (Bonasoni et al., 2010; Decesari et al., 2010; Marinoni et al., 2010). In addition, studies have shown the obstruction of flow caused by the high Himalaya which intensifies the effect of pollution over the IGP that are visible in satellite imagery especially during pre-monsoon seasons (Singh et al., 2004; Dey and Di Girolamo, 2010; Gautam et al., 2011). Though there is evidence of existence of similar source pollutants, both regional and local, in the foothills and the higher altitude sites (Raatikainen et al., 2017; Raatikainen et al., 2014; Srivastava et al., 2012,), observational evidence of mechanisms and pathways facilitating such transport via Himalayan valleys is lacking. Our data fills this gap by characterizing the role of the wind system within a deep Himalayan valley in transporting pollutants from the IGP to the high mountains.”

Page 4, line 133: actually, the intrusion of the haze is not so visible from Figure 1a.

The image in figure 1a has been zoomed in to better show the intrusion of haze.

Page 4, line 138: the description of the valley orientation is difficult to follow. Some of the described features (e.g. Eastward orientation at Jomstom) cannot be captured by Figure 1. I would suggest to add to Figure 1 a more detailed map of the measurement site.

We have replaced table 1 with a new figure 2, which includes a clear map of the valley.

Page 5, line 148: please add to Table 1 a column with measured parameters

The measured parameters are now included in the new figure 2.

Page 5, line 151: actually “equivalent BC” is measured by MAAP.

The text now reads:

“Equivalent black carbon (hereafter referred to as BC)...” is specified when first used and, for efficiency, the acronym BC is used thereafter.

Page 5, line 158: please substitute “attenuation” by “absorption”. For O₃ and eqBC, please provide indication about measurement uncertainty and QA/QC procedures.

We have changed attenuation to absorption. Additional description on QA/QC procedures have been added.

Page 5, line 161: please indicate the percentage of data available over the period January 2013 – August 2015. Please, remove the sentence “Measurements of carbon monoxide. . .” (no CO data were presented/discussed in the paper).

A data timeline has been added as supplementary table 1 and we have removed CO measurements from the sentence.

Page 5, line 164: no winter season has been identified?

Our analysis focused on variability in BC and O₃ variability during wet (monsoon) and dry (pre-monsoon and post-monsoon) seasons. Consequently, identification and interpretation of variability during the winter season was not directly relevant.

Page 5, line 169: I would skip “about 10 meters above and”

We prefer to retain the clarification that meteorological parameters were measured 10 meters above ground to ensure that readers know that AWS were above the surface layer.

Page 5, line 175: I cannot understand this kind of normalization. Why did you not report actual eqBc and O₃ values? You should simply report the averaged seasonal diurnal variation of O₃ and eqBC obtained by subtracting averaged monthly values from hourly values.

The approach we employ here to characterize diurnal variability normalizes for day-to-day variability in concentrations, quantitatively captures the frequency distributions in normalized cycles, and is widely used in the literature (e.g., Sander et al., 2003, ACP; Fischer et al., 2006; JGR, Keene et al., 2007, JGR; Smith et al., 2007, JGR, Young et al., 2013, JGR; among others). Cycles derived from average values typically dampen the relative range of actual diurnal variability.

Figure 2: I would like to see the percentiles for each single month. This would provide also information about year-to-year variability.

Figure 2 in the submitted version of the manuscript depicts percentile distributions based on data binned into each month over the duration measurement period. These results were interpreted to evaluate seasonal variability. While we agree with the reviewer that it would be interesting to evaluate year-to-year variability, the limited duration of the measurement period, 2.5 years, is insufficient for a reliable analysis of this nature.

Page 6, line 189: please provide references. Possible reduced domestic emissions related to less domestic heating?

We have added the references and clarified the text. It reads as follows:

“We infer that the significantly lower concentrations during the monsoon reflect the influences of synoptic easterly airflow that transports cleaner marine air mass over the region, reduced agricultural residue burning (Sarangi et al., 2014), and more efficient removal via wet deposition (Dumka et al., 2010).”

Page 6, line 197: “Seasonal variability. . .broad regional pattern”. I do not agree. In the IGP, BC is maximized during winter months (December- January), while in Himalayas (and also at your station) the values are higher during pre-monsoon! (see also).

We agree with the reviewer and recognize that BC peaks during Dec-Jan in the IGP and during March- May in the Himalayan sites. We have clarified the language in section 3.1 as follows:

“Similar seasonal variability in BC concentration is evident across the IGP from urban to remote locations. For example, high concentrations of BC (~1.48 to 1.99 $\mu\text{g m}^{-3}$) have been reported in near-surface air across the IGP as well as in layers of the atmosphere at ~900 m asl and ~1200 m asl during the post-monsoon over Northern India (Tripathi et al, 2005; 2007). Sreekanth et al (2007) reported BC concentrations in Vishakhapatnam, in eastern India, to be 8.01 $\mu\text{g m}^{-3}$ in pre-monsoon and 1.67 $\mu\text{g m}^{-3}$ during monsoon while Ramchandran et al (2007) observed BC concentrations in Ahmedabad, western India, of 0.8 $\mu\text{g m}^{-3}$ during the monsoon in July to 5 $\mu\text{g m}^{-3}$ during the post monsoon in January. Similar seasonal variability has also been reported in the high Himalaya. For example, the Nepal Climate Observatory-Pyramid (NCO-P) station at the 5079 m asl in the Himalaya has also shown high seasonal differences for BC (0.444 (± 0.443) $\mu\text{g m}^{-3}$ during pre-monsoon and 0.064 (± 0.101) $\mu\text{g m}^{-3}$ during monsoon season and ozone concentrations 61 (± 9) ppbv during pre-monsoon season and 39 (± 10) ppbv during monsoon (Cristofanelli et al., 2010, Marinoni et al., 2013) (Supplementary Table 2). Our results indicate that seasonal variability in BC and O₃ within the KGV and presumably other deep Himalayan valleys is coupled with these larger regional-scale patterns.”

Page 6, line 209: “These differences in. . .”. Not clear: what differences?

This point is addressed in our response to the preceding comment.

Page 6, line 213: The works by Ratikainen et al., 2014 AtmosEnv can be cited here

We have added a citation to this study in the revised version.

Section 3.2: this discussion is mainly qualitative. No statistical analysis have been applied and it is difficult to discern if the observed features are statistically significant. I suggest to add a line describing the mean average values with statistical confidence level (this would help in understand if the observed peak and minima are robust features). I would add to these plots the

analogous for wind direction and speed to clearly correlate wind regime with O₃ and eqBC variability. In any case, the results are based just on the analysis of 3 single months of observations. A comment for taking into account the possible intra-seasonal and year-to-year variability should be added. Your measurement period is 2.5 year-long. Why you did not use all the available data?

Figure 2 of the original version of the manuscript (Figure 3 of the revised version) depicts monthly percentile distributions for both BC and O₃ over the entire measurement period. As indicated in the Section 3.2 (lines 190 to 192 of the original manuscript), “representative months from each season, April 2013 (pre-monsoon), July 2015 (monsoon) and November 2014 (post-monsoon), were selected based on data availability and quality to evaluate aspects of temporal variability in more detail.” Normalize diurnal variability in concentrations of O₃ and BC during these months is depicted in Figure 3 of the original version (Figure 4 of the revised version). The role of wind in the transport is discussed in section 3.4. As mentioned in response to a previous comment, a 2.5-year data record is insufficient to reliably characterize inter-annual variability particularly given the data gaps in our study.

In addition, we have added results from non-parametric statistical analysis that shows differences between up-valley and down-valley concentration and flux. For this analysis we have used all days during the measurement period when 24 hour data for all parameters measured were available. As the data is not normally distributed a mean average value, as suggested, are not appropriate to evaluate significant differences day and night.

Page 7, line 219: “peaked in the early afternoon”. I would say “at noon”! This can be an hint for local photochemical production. . .

The peak is too broad to assign specific time of the day. For this reason, we prefer to retain use of the term “early afternoon”.

Page 7, line 220. “Finally, . . . 0 to 1 (Fig. 3)”, I cannot be able to understand this sentence. . . Maybe you would suggest that diurnal variability account for the most part of the overall O₃ variability? In the case, this is a point that should be better stressed. Can you quantify it?

We have clarified this sentence to read; “In contrast, based on median values during all three periods, BC concentrations increased rapidly in the early morning, decreased during late morning, and then rose through the afternoon and early evening hours (Fig. 5).”

Page 7, line 223: “increased rapidly following sunrise”. . . because later in the manuscript, you suggested that this peak can be related to local emissions, I would change with “increased rapidly in the early morning”.

We have made the recommended change.

Page 7, line 225-229: Again, this sentence is not clear to me. See the same comment for ozone.

We have clarified the text to read; “Notably, BC concentrations showed lower variability relative to that of O₃, particularly during pre-monsoon periods. These skewed distributions reflect infrequent periods of relatively high BC concentrations during all three seasons.”

Page 7, line 230: you should also mention air-mass transport. At a remote site, if local emissions are really negligible (I’m not totally convinced about this for your site, see your following sentence about eqBC), I would expect that the contribution by transport is the most important one!

We have provided further clarification, the text now reads:

“Several factors contributed to differences in the diurnal variability of O₃ and BC. These include diurnal variability in emissions of BC versus O₃ precursors and/or production in source regions followed by regional transport, diurnal variability in the photochemical chemical production and destruction of O₃ and contributions of O₃ from non-combustion sources. O₃ is produced photochemically and is lost via deposition to surfaces and chemical reactions. In contrast, BC is a primary emission product of combustion that may originate from both local and distant sources.”

We have also added text as further evidence that these emissions are not local. (See response to following comment)

Page 7, line 236: the secondary peak (in the evening from 19 to 21) is visible only during the post-monsoon. Please comment. Does this peak be related with domestic emissions (e.g. domestic cooking or heating)?

The contribution from local pollutants dominate morning peaks while the influx of pollutants after the onset of up-valley flows suggest long-range transport. The absence of secondary peak during monsoon season supports the argument. The peaks are present both during pre-monsoon and post-monsoon seasons (old figure 6). This has been clarified in the text to read;

“The early morning peak during all three seasons suggests probable contributions from the local combustion of biofuels for cooking and heating, which are most prevalent during early morning. The secondary peak in the afternoon and early evening occur when the local anthropogenic sources are at minimum in the KGV.”

Page 7, line 239: “Up-valley. . .Alpine pumping”. As mentioned before, many works in Himalayas investigated the role of valleys as channel of anthropogenic pollution. Please consider them and comment your results as a function of these previous works.

We have included additional references to recent papers that have investigated pollution transport in the Himalaya throughout the manuscript. Some of these studies have examined this pathway through satellite imagery and remote sensing. Others have made field-based measurements in the IGP and TP. However, as stated in the manuscript, ours is the first study to directly measure air pollution transport within a trans-Himalayan valley. We have also added a table that compares our results with results from Bonasoni (2010)

Section 3.3: the expected outcome from this Section is not clear. Why did you show just 6 days of data at JSM_2, when more than two years of meteorological data are available at the “core” site where also O₃ and eqBC data were available? You must show these data! Moreover, if I’m not wrong, JSM_2 is located 1000 m above the “core” site. Thus, which is the goal of showing these data?

In the original manuscript, the station names at Jomsom were in misplaced. These errors have been corrected and we apologize for any related the confusion.

We have updated the old wind rose figure with wind roses for JSM_2 for all seasons (new figure 6a) binned every three hours for the duration of the measurement period. The wind roses show the seasonality in wind direction and magnitude of wind speed at Jomsom.

Section 3.4: Legend is missed in Figure 6. I suspect that blue dots represent O₃ but you have to add a legend! Basically, this section repeat the same concept about diurnal variability already reported by Section 3.2. . .

The legend has been added. Section 3.2 describes the diurnal variability in the BC and O₃ concentrations. Section 3.3 describes the wind pattern in the valley. Building on these lines of evidence, section 3.4 describes how BC and O₃ concentration variability correlates with wind variability. It is important to state this link explicitly before we describe the anomalies we observe in diurnal concentration (section 3.5).

Page 8, line 271: “This peak occurred about an (one) hour later during the post-monsoon period”. Looking at Figure 3, this seems not true! eqBc peak at 8:00 AM during all the seasons. However, it is important to evaluate the robustness and origin of this peak. Looking at the eqBc time series reported in Figure 6, it looks that the early morning peak is related to “spiky” observations, very likely related to local emissions. This is particularly evident during post-monsoon, when these “spikes” were observed during the diurnal minima of eqBC. This feature can be of a certain interest to evaluate the local emissions to the “pristine” Himalayan environment, but I would neglect it for the analysis of transport processes affecting O₃ and eqBC variability.

Please refer to the response earlier to the comment about secondary peaks.

Page 8, line 275: “. . .decreasing concentration with increasing wind speeds are consistent with expectation based on dilution”. I think that the decrease on eqBC observed during midday can be associated not only to dilution in a more developed PBL of local emissions, but also to the fact that air-masses reaching the site from the lower valley are still not enriched in pollutant. . . Indeed, you observed eqBC (and O₃) increase in the afternoon/evening (when both PBL height decrease and air-masses richer in pollution could reach the site from longer distance). You should roughly evaluate the distance of eqBC emissions by analysing wind speed at the measurement sites. . .

We have roughly calculated the maximum distance from which the secondary peak emissions could have originated during May 2015. We estimate that emissions could have traveled from as far as 70km away from Lete. This estimate was done by calculating the time it would take for the secondary peak occurring at Jomsom (1900 LST) to travel from Lete (1810 LST) to Marpha (1850 LST) to Jomsom. We then determined the difference in time (8 hours) between when emissions started to increase after the morning peak at Jomsom and the occurrence of the secondary peak at Jomsom. Finally, we used this 8 hour estimate combined with wind speed measurements at Lete to calculate the maximum distance from Lete from which secondary peak emissions could have originated. This poorly constrained estimate does not account for other factors that influence pollutant transport and its reliability cannot be evaluated based on objective criteria. Consequently, we choose not to include it in our paper.

Page 8, line 285. This detailed description of local wind regime needs a more detailed map on Figure 1!

The revised manuscript includes a more detailed map (new figure 2).

Page 9, line 294: “Nocturnal decoupling of the boundary layer preserves the concentration of. . .”. Not clear: what do you mean with “decoupling PBL”? Decoupling from what?

Author: *We have removed the sentence.*

Section 3.4: I assume that this Section should be “Evidence of LONG-RANGE transport episodes. . .”. In this section you discuss three typical regimes of O₃ and eqBC variability. However, I would like to see a more detailed description of the main features of each single regime (basically how are you able to distinguish among them?) and a systematic assessment of their occurrence and impact on eqBC and O₃ variability E.g. which is the frequency of occurrences of these regimes on a seasonal basis? Are you able to objectively identify (by some

selection criteria) the occurrence of that regimes? Can you able to compare your results with previous studies? (e.g. Putero et al., Environ. Poll. 2013)

We have changed the section title to “Evidence of regional transport episodes”. We also updated the figure with wind data for the episodes shown as examples (new figure 8); have quantified the frequency of each transport pattern and included all the transport pattern observed in supplementary table ..

Page 9, line 304: actually you did not show any evidence of transport to TP! I think this is just a (reasonable) speculation. Maybe you can discuss this possibility in the conclusions Section.

We have added transport to TP in the conclusion as a potential transport to the TP.

Page 9, line 310: I think that the relationship between eqBc , O3 and fire emissions in the IGB is only qualitative and deserve more analyses. At least a correlation between the temporal variation of the fire number in the IGP and the eqBc and O3 at the measurement site must be showed. Moreover, air-mass transport analysis (i.e. backtrajectories or dispersion plume) corroborating the transport towards the measurement site region should be showed (the same is valid for case B). For case B and C, eqBc is maximized during night-time, when down-valley winds are expected in a mountain valley and cleaner air-masses from upper layers should be present (add the behaviors of wd and ws!). Please, comment. Moreover, the different co-variability (correlation) between O3 and eqBC should be better investigated and commented. During case B, the diurnal variability of O3 and eqBC appeared to be minimized. Can this indicate the role of far (fires?) emissions instead of regional/local ones? The increase of daytime minima value of eqBc and O3, would indicate a build-up of pollution. Is this build-up only limited to the valley or did it extend to the foothills? Maybe time series of satellite MODIS data can help. . .

The authors feel that back trajectories trying to relate surface sources to valley transport are unreliable in complex terrain so we used HYSPLIT back trajectories from the mouth of the valley in conjunction with the MODIS imagery. The back trajectories show transport of air mass from are with high biomass/ forest fires activity and/or haze over the IGP during the regional transport period examples. It supports the hypothesized source for the high concentration during regional transport episode. Dispersion models are beyond the scope of this paper.

Section 3.4.2 is confused and not provides important information: thus, it can be skipped. STE discussion at this point is a little bit out of the scope of the paper. A rigorous assessment of STE contribution to eqBC and O3 variability would deserve a specific investigation. Moreover, I would note that the focus on the monsoon season is of limited interest, since it is well assessed

that summer monsoon is the season during which transport of stratospheric air-masses to the lower troposphere is minimized over the Himalayan region (see e.g. Putero et al., 2016, Ohja et al., , 2016).

We have removed discussion of STE from the paper.

The conclusions are not robust. Actually you did not demonstrate the transport of pollutant from IGP to TP but just the transport of pollution up to the valley. Your main results (seasonal and diurnal O₃ and eqBC variability, influence of open fires) should be better commented in the framework of the most recent studies on the topic.

In response to the reviewer's comment regarding transport to the TP, we have revised the text to indicate that that our observational evidence suggests (but does not conclusively demonstrate) such a connection.

Referee #2

The manuscript reports data that is collected recently over a high altitude site and does not bring in any new insights or results. As the authors write, many results from the same group have been published recently.

Numerous studies have looked at the possibility of the transport of pollutants from the IGP to the Himalayan foothills (Pant et al., 2006; Dumka et al., 2008; Komppula et al., 2009; Hyvärinen et al., 2009, 2010; Ram et al., 2010; Brun et al., 2011; Gautam et al., 2011; Srivastava et al., 2012b). In addition, the obstruction of flow caused by the high Himalaya intensifies the effect of pollution over the IGP that are visible in satellite imagery especially during pre-monsoon seasons (Singh et al., 2004; Sarkar et al., 2006; Bollasina et al., 2008; Gautam et al., 2009; Dey and Di Girolamo, 2010). Other studies show that pollutants, with similar regional sources, have the potential to reach not only the foothills of the Himalaya but also higher elevations (Decesari et al., 2010; Marinoni et al., 2010; Sellegri et al., 2010; Gobbi et al., 2010). Though there is evidence of existence of similar source pollutants, both regional and local, in the foothills and the higher altitude sites (Raatikainen et al., 2016, Raatikainen et al., 2014, Srivastava et al., 2012,), observational evidence of mechanisms and pathways facilitating such transport is lacking. Our data fills this gap by characterizing the role of the wind system within a deep Himalayan valley in transporting pollutants from the IGP to the high mountains.

These data have not been previously published.

What is the relevance of connecting ozone and BC is not clear. Many aspects are very loosely dealt with and mentioned in passing. References are missing.

The rationale for investigating BC and ozone is explained in detail in the introduction. Briefly, both species are short-lived climate forcers (SLCFs) that originate from combustion sources over the IGP. We measured these species in conjunction with corresponding meteorological conditions and satellite imagery to understand the importance of deep valleys in their transport to the high Himalaya. Impacts on ice-albedo and temperature contributes to warming, which accelerated melting of glaciers with potential negative consequences for almost a billion people in the surrounding watersheds. Mitigation of SLCF emissions has the potential to slow the rate of future climate change. As indicated in our responses to comments by Reviewer 1, we have added references relevant to the analysis.

Lines 285 - how this phenomenon can occur? What about lifetime of BC aerosols?

As indicated above in our response to a similar comment by Reviewer 1, we roughly estimated the transport time required for an air mass from Lete to Jomsom (approximately 50 minutes) and the distance of the source from Lete (approximately 70km). Given the lifetime of BC and in the absence of substantial wet or dry deposition, emissions from IGP could reach Lete and up the KGV under suitable synoptic and local weather.

Conclusion - with the limited scope of the study the conclusions are far fetched.

While the reviewer was not specific regarding the nature of his/her concern, we have exercised greater caution in the statements regarding transport of pollutions from the IGP to the TP and revised the conclusion section. It now reads,

“This study provides in-situ observational evidence of the role of a major Himalayan valley as important pathway for transporting air pollutants from the IGP to the higher Himalaya. We found that:

- Concentrations of BC and O₃ in the KGV exhibited systematic diurnal and seasonal variability. The diurnal pattern of BC concentrations during the pre- and post-monsoon seasons were modulated by the pulsed nature of up-valley and down-valley flows. Seasonally, pre-monsoon BC concentrations of BC were higher than in post-monsoon season.*
- The morning and afternoon peaks in the post monsoon season was more pronounced than those of pre-monsoon season likely due to the relatively lower wind speeds during post-monsoon.*

- *When compared to a high elevation site, NCO-P CNR in the Himalaya, JSM_STA consistently showed higher BC concentrations for all seasons whereas the corresponding O3 concentrations were higher at NCO-P CNR.*
- *Significant positive up-valley fluxes of BC were measured during all seasons.*
- *During episodes of regional pollution over the IGP, relatively higher concentrations of BC and O3 were also measured in the KGV.*

Further studies are needed to understand the vertical and horizontal distribution of particulate matter and ozone in the Himalayan region, and their impact on the radiative budget, the ASM and climate. Investigations using sondes, LiDar and air-borne measurements could help characterize the stratification of the vertical air masses.”

Transport of regional pollutants through a remote trans-Himalayan valley in Nepal

Shradda Dhungel¹, Bhogendra Kathayat², Khadak Mahata³, Arnico Panday^{1,4}

¹ Department of Environmental Sciences, University of Virginia, Charlottesville, VA 22904, USA

² Nepal Wireless, Shanti Marg, Pokhara, 33700, Nepal

³ Institute for Advanced Sustainability Studies, Potsdam, 14467, Germany

⁴ International Center for Integrated Mountain Development, Khulmaltar, Kathmandu, 44700, Nepal

Correspondence to: Shradda Dhungel (shradda@virginia.edu)

Abstract. Anthropogenic emissions from the combustion of fossil fuels and biomass in Asia have increased in recent years. High concentrations of reactive trace gases and absorbing and light-scattering particles from these sources over the Indo-Gangetic Plain (IGP) of southern Asia form persistent haze layers, also known as atmospheric brown clouds, from December through early June. Models and satellite imagery suggest that strong wind systems within deep trans-Himalayan valleys are major pathways by which pollutants over the IGP are transported to the high Tibetan Plateau (TP). To evaluate this pathway, we measured black carbon (BC), ozone (O₃), and associated meteorological conditions within the Kali-Gandaki Valley, Nepal, from January 2013 to August 2015. BC and O₃ varied over both diurnal and seasonal cycles. Relative to nighttime, mean BC and O₃ concentrations within the valley were higher during daytime when the up-valley flow (average velocity of 17 ms⁻¹) dominated. Minimal BC and O₃ concentrations occurred during the monsoon season (July to September). Concentrations of both species subsequently increased post monsoon and peaked during March to May. We recorded average concentration for O₃ during April, July, and November were 41.7 ppbv, 24.5 ppbv, and 29.4 ppbv, respectively, while the corresponding BC concentrations were 1.17 μg m⁻³, 0.24 μg m⁻³, and 1.01 μg m⁻³, respectively. Frequent episodes of concentrations two to three fold higher than average persisted from several days to a week during non-monsoon months. [Our observations of increases in BC concentration and fluxes in the valley, particularly during preceding the monsoon and in conjunction with widespread agricultural burning and wildfires over the IGP, support the hypothesis that trans-Himalayan valleys are important conduits for transport of pollutants from the IGP to TP.](#) **Keywords:** [black carbon, ozone, trans-Himalayan valleys, pollutant pathways, long-range transport, regional transport episodes, short-lived climate forcers.](#)

[Our observations of increases in BC concentration in the valley—especially during pre-monsoon season \(April\)—support the hypothesis that trans-Himalayan valleys are important conduits for transport of pollutants from the IGP to TP. In addition, the increase in BC concentration in the KGV during high fire activity in Northern India and southern Nepal corroborates the role of trans-Himalayan valleys as vital pollutant transport pathways.](#)

Keywords: black carbon, ozone, trans-Himalayan valleys, pollutant pathways, long-range transport, regional transport episodes, short-lived climate forcers.

1. Introduction

Persistent atmospheric haze, often referred to as Atmospheric Brown Clouds (ABC) (Ramanathan and Crutzen, 2003), affects broad geographic regions including the Indo-Gangetic plain (IGP) in southern Asia (Ramanathan and Carmichael, 2008), eastern China (Ma et al., 2010), southeast Asia (Engling and Gelencser, 2010), sub-Saharan Africa (Piketh et al., 1999), Mexico (Vasilyev et al., 1995), and Brazil (Kaufman et al., 1998). In southern Asia, the haze covers extensive areas particularly during the period of mid-November to mid-June that precedes the summer monsoon season. Major combustion sources (primarily anthropogenic) including wildfires and the burning of agricultural waste, garbage, biofuel, and fossil fuels emit volatile and particulate-phase compounds to the atmosphere that contain oxidized and reduced forms of sulfur, nitrogen, and organic carbon (OC) together with elemental (black) carbon (BC) and minerals. These emissions are intermixed and chemically interact with mechanically produced aerosols (e.g. sea salt and mineral dust). Important secondary pollutants such as ozone (O₃) from photochemical reactions involving nitrogen oxides are also produced. Together, this mixture of atmospheric species constitutes ABC or the brown haze in South Asia (Ramanathan et al., 2005; Gustafsson et al., 2009). These optically thick layers include high concentrations of light absorbing and light scattering particles (Menon et al., 2002) that modulate radiative transfer. Light absorbing aerosols (primarily BC and mineral dust) contribute to warming of the atmosphere while light scattering aerosols (primarily S-, N-, and OC dominated particles) drive cooling at the surface.

The combined effects of light absorbing and light scattering aerosols from anthropogenic sources reduce UV and visible wavelength radiation at the surface (i.e., surface forcing), increase the warming of the troposphere (i.e., atmospheric forcing) and change the net top of the atmosphere solar flux (i.e., top-of-the-atmosphere forcing) (Andreae and Crutzen, 1997; Kaufman et al., 2002, Ramanathan et al., 2005). Absorbing anthropogenic pollutants like BC significantly influence global warming, in terms of direct radiative forcing (Jacobson, 2001; Bond et al., 2013); regional influences from such pollutants close to sources are greater than those on the global scale (Ramanathan et al., 2007b).

The combined effects of light absorbing and light scattering aerosols from anthropogenic sources reduce UV and visible wavelength radiation at the surface (i.e., surface forcing), increase the warming of the troposphere (i.e., atmospheric forcing) and change the net top of the atmosphere solar flux (i.e., top-of-the-atmosphere forcing) (Andreae and Crutzen, 1997; Kaufman et al., 2002, Ramanathan et al., 2005). Absorbing anthropogenic pollutants like BC significantly influence global warming, in terms of direct radiative forcing (Jacobson, 2001); regional influences from such pollutants close to sources are greater than those on the global scale (Ramanathan et al., 2007b). Ozone precursors including nitrogen oxides and volatile organic carbon (VOC) are emitted to the atmosphere together with BC from combustion sources. VOCs are also emitted from biogenic sources including microbial decomposition and vegetation. In addition, the downwelling of stratospheric ozone across the tropopause contributes to

75 ~~background levels of tropospheric O₃. Finally, O₃ is produced photochemically during the daytime whereas BC is a relatively inert primary emission product.~~

80 The elevated concentration of aerosols in the anti-cyclone weakens the circulation pattern and reduces total monsoon precipitation over southern India (Ramanathan et al, 2005; Fadnavis et al., 2013) while intensifying the monsoon over the foothills of the Himalaya (Lau et al., 2006). In addition to warming the atmosphere, the rising concentrations of BC and O₃ over southern Asia (e.g., Ramanathan and Carmichael, 2008) have detrimental impacts on human health. The effects of BC on cardiopulmonary and respiratory problems are greater than those of PM 2.5 or 10 particles (Janssen et al., 2011). O₃ also compromises pulmonary function (Krupnick et. al, 1990) and is a leading pollutant causing biodiversity loss (Royal Society, 2008) and declining crop yields by directly damaging leaves (Auffhammer et al., 2006).

85 ~~Air pollution from the source regions across the IGP, which extends along the southern side of the Himalaya from eastern Pakistan across northern India and southern Nepal to Bangladesh, often reach heights of more than 3 km above sea level via convection and advection (Ramanathan et al., 2007a). The radiative properties of associated aerosols influence the Asian summer monsoon (ASM) (Lau et al., 2006). The elevated concentration of aerosols in the anti-cyclone alters the strength of circulation pattern and reduces total monsoon precipitation over southern India (Ramanathan et al, 2005; Fadnavis et al., 2013) while intensifying the monsoon over the foothills of the Himalaya (Lau et al., 2006). BC and O₃ concentrations are rising in response to increasing emissions over southern Asia (Ramanathan and Carmichael, 2008). In addition to warming the atmosphere, both pollutants also have detrimental impacts on human health. The effects of BC on cardiopulmonary and respiratory problems are greater than those of PM 2.5 or 10 particles (Janssen et al., 2011). O₃ also compromises pulmonary function (Krupnick et. al, 1990) and is a leading pollutant causing biodiversity loss (Royal Society, 2008) and declining crop yields by directly damaging leaves (Auffhammer et al., 2006).~~

100 Most haze over the IGP is in the lower 3 km of the atmosphere, and the Himalaya range forms a 2500 km long complex topographic barrier along the northern edge of the IGP extending more than 8 km high. However, satellite imagery (Ramanathan et al., 2007a), back trajectories (Lu et al., 2011), model calculations (Kopacz et al., 2011), and ice core analyses (Lee et al., 2008, Kang et al., 2010) strongly suggest that pollutants are efficiently transported from the IGP to the Tibetan Plateau (TP), especially during spring prior to the monsoon. Absorbing aerosols warm the atmosphere at high altitudes and Aerosols from the IGP significantly impact the Himalaya and TP. Absorbing aerosols warm the atmosphere at high altitudes and, when deposited onto snow and ice surfaces, decrease albedo thereby substantially increasing the rate of glacial and snow melting (Kang et al., 2010). Model simulations (Qian et al., 2011) show that the absorbing aerosols change the surface radiative flux in the higher Himalaya and the TP by 5 to 25 W m⁻² during the pre-monsoon months of April and May. Atmospheric and surface absorption of solar radiation drives the physical climate system and the associated biogeochemical cycles that sustain life on the Earth. The TP plays a vital role in regulating the regional

climate due to its effect on the Asian summer monsoon (ASM) and the hydrologic cycle. The interrelated perturbations of the ABC on radiative transfer, air quality, the hydrologic cycle, and crop yields have important long-term implications for human health, food security, and economic activity over southern Asia. The TP plays a vital role in regulating the regional climate due to its effect on the ASM and the hydrologic cycle. High atmospheric mixing ratios of O₃ during growing seasons can decrease yields of wheat, rice and legumes in regions with increased O₃ pollution (Wang and Mauzerall, 2004). The interrelated perturbations of the ABC on radiative transfer, air quality, the hydrologic cycle, and crop yields have important long-term implications for human health, food security, and economic activity over southern Asia.

Lüthi et al. (2015) found that synoptic circulation patterns, in combination with local weather phenomena, are associated with the transport of polluted air masses from the IGP to the TP. Several major Himalayan valleys including the Arun Valley in eastern Nepal and the Kali Gandaki Valley (KGV) in western Nepal provide topographical connections for air masses from the south to the TP (Fig.1). In addition to synoptic transport over the Himalaya, MODIS (MODerate-resolution Imaging Spectroradiometer) and CALIPSO (Cloud-Aerosol Lidar and Infrared Pathfinder Satellite Observation) imagery reveal northward slanted transport of polluted air mass towards higher elevations in the Arun Valley (Brun et al., 2011). However, to date, there has been little research to understand the role of mountain valleys on how air pollutants from the IGP and the Himalayan foothills flow through the topographic barrier. Well-known flow patterns carry polluted air masses up valleys to higher elevations by providing a path of least resistance between tall mountains. However, to date, there has been little research on how air pollutants from the IGP and the Himalayan foothills cross the topographic barrier to reach the TP. Even during the absence of strong synoptic patterns, satellite imagery show IGP haze penetrating deep into mountain valleys on the south side of the Himalayan range (Brun et al., 2011). Well-known flow patterns carry polluted air masses up valleys to higher elevations by providing a path of least resistance between tall mountains. In the European Alps, prevailing wind systems in the mountain river valleys funnel polluted air from peripheral source regions to high elevations in a phenomenon known as “Alpine Pumping” (Weissmann et al., 2005). Under fair weather conditions during daytime, the upslope winds are capable of transporting significant pollutants and moisture into the free troposphere (Henne et al., 2004). Relative to air over plains, the air within the valleys heats and cools more quickly (Steinacker, 1984). The resultant differences in temperature create gradients in pressure and air density, which in turn drive the wind that transports air from the plains to higher-elevations during the daytime (Reiter and Tang 1984, Whiteman and Bian, 1998; Egger et al., 2000).

Numerous studies have investigated the possibility of the transport of pollutants from the IGP to the Himalayan foothills (Pant et al., 2006; Dumka et al., 2008; Komppula et al., 2009; Hyvärinen et al., 2009; Ram et al., 2010; Brun et al., 2011; Gautam et al., 2011; Srivastava et al., 2012). Other studies show that pollutants have the potential to reach not only the foothills of the Himalaya but also higher elevations (Bonasoni et al., 2010; Decesari et al., 2010; Marinoni et al., 2010). In addition, studies have shown the obstruction of flow caused by the high Himalaya which intensifies the effect of pollution

150 over the IGP that are visible in satellite imagery especially during pre-monsoon seasons (Singh et al.,
2004; Dey and Di Girolamo, 2010; Gautam et al., 2011). Though there is evidence of existence of
similar source pollutants, both regional and local, in the foothills and the higher altitude sites
(Raatikainen et al., 2017; Raatikainen et al., 2014; Srivastava et al., 2012.), observational evidence of
mechanisms and pathways facilitating such transport via Himalayan valleys is lacking. Our data fills
155 this gap by characterizing the role of the wind system within a deep Himalayan valley in transporting
pollutants from the IGP to the high mountains. Several major trans-Himalayan valleys including the
Arun Valley in eastern Nepal and the Kali Gandaki Valley (KGV) in western Nepal provide
topographical connection for air masses from the south to the TP (Fig.1). In addition to synoptic
transport over the Himalaya, MODIS (MODerate-resolution Imaging Spectroradiometer) and
160 CALIPSO (Cloud-Aerosol Lidar and Infrared Pathfinder Satellite Observation) imagery reveal
northward-slanted transport of polluted air mass towards higher elevations in the trans-Himalayan Arun
Valley (Brun et al., 2011). The KGV exhibits distinct diurnal wind pattern, with strong daytime up-
valley flow and weak nighttime down-valley flow. Based on the average daytime wind speed, the valley
is divided into three regions: the entrance, core, and exit (average wind speeds range from 5 to 10 m s⁻¹,
165 8 to 18 m s⁻¹, and less than 5 m s⁻¹, respectively) (Egger et al 2000). The strongest winds within the core
region are most prevalent in the lower 1000 to 1500 m of the boundary layer in the valley (Egger et al,
2000; Züngl et al., 2000, Egger et al., 2002).

In 2011 we established an atmospheric measurement station in Jomsom (28.87° N, 83.73° E, 2900 m
asl) within the core region of the KGV along with automated weather stations up and down the valley
170 from Jomsom. With the exception of aerosol optical depth measured as part of AERONET (AErosol
RObotic NETwork) (Xu et al., 2015), no data from Jomsom have been reported previously. Here we
report diurnal and seasonal trends in two climatically important pollutants — BC and O₃. Results are
interpreted to evaluate the role of trans-Himalayan valleys as pathways for the transport of polluted air
from the IGP to the TP.

175 2. Measurement Sites and Methods

2.1 Measurement Sites and Instrumentation

This paper presents data from an atmospheric measurement station in Jomsom (28.87° N, 83.73° E,
2900 m asl) within the core region of the KGV along with automated weather stations up and down the
180 valley from Jomsom. With the exception of aerosol optical depth measured as part of AERONET
(AErosol RObotic NETwork) (Xu et al., 2015), no pollution data from Jomsom have been reported
previously. Here we report diurnal and seasonal trends in two climatically important pollutants – BC
and O₃. Results are interpreted to evaluate the role of trans-Himalayan valleys as pathways for the
transport of polluted air from the IGP to the higher Himalaya.

185 The KGV is located in the Dhaulagiri zone of western Nepal. Figure 1(a), shows the TP in the upper
right, with the Himalayan arc, the Himalayan foothills of India, Nepal and Bhutan, and the haze covered
IGP to the south. The intrusion of haze from the IGP into Himalayan valleys is clearly visible. KGV
190 floor changes elevation from approx. 1100 m to 4000 m asl over a horizontal distance of 90 km (Fig.
1(b)). Passing between the two eight thousand meter peaks of Dhaulagiri and Annapurna, it forms one
of the deepest valleys in the world. The valley is a narrow gorge at the lower end and opens up into a
wider, arid basin half way up (Fig. 1(b)). The maximum width of the basin is approximately one
kilometer. The orientation of KGV varies from the entrance to the exit. The valley is oriented
southeasterly (~135°) to northwesterly (~315°) at the bottom. The valley's orientation changes to
southwesterly (~225°) to northeasterly (~45°) at the core of then turns north (~20°) past the core of the
195 valley (Fig. 1). The orientation of KGV varies from the entrance to the exit. The valley is oriented
southeasterly (~135°) to northwesterly (~315°) at Lete. The valley's orientation changes to
southwesterly (~225°) to northeasterly (~45°) at Marpha. At Jomsom, the valley bends towards the east
(~210°) and past Eklabhatti the valley turns north (~20°) (Fig. 1). Approximately 13,000 inhabitants in
several small settlements sparsely populate the valley. Emission sources within the valley include
200 biofuel combustion for cooking and fossil-fuel combustion by a few scattered off-road vehicles. A total
of 5245 vehicles have been registered in Dhaulagiri Zone since 2008, but most are based in the southern
towns of Kusma, Baglung, and Beni, below 1 km altitude, at the lowest left corner of the map in Figure
1(b) (DOTM, 2016).

The atmospheric observatory at Jomsom (JSM_STA) is equipped with instruments to measure BC, O₃,
205 ~~carbon monoxide, aerosol optical depth,~~ and meteorology (Table 1). The observatory is located on the
southeast corner of a plateau jutting out from an east-facing slope about 100 m above the valley floor
and with no major obstructions either up or down the valley.

. Equivalent black carbon (hereafter referred to as BC) BC was measured with a Thermo Multiangle
Absorption photometer (MAAP), model 5012 that analyzes the modification of radiation fields in the
210 forward and back hemisphere of a glass-fiber filter caused by deposited particles using a multi-angle
photometer. MAAP was operated at a flow rate of 20 L min⁻¹ and measures BC at 1-minute frequency.
Hyvarinen (2013) illustrates the artifact in MAAP measurements in environments with high aerosol
loading with an underestimation of concentration above 9 µg m⁻³. Since the median monthly
concentration were less than 1 µg m⁻³ and 90th percentile below 2 µg m⁻³ for all seasons which is below
215 the threshold of 9 µg m⁻³, MAAP corrections were not applied. O₃ was measured with a 2B Tech model
205 via the attenuation of ultraviolet light at 254 nm passing through a 15 cm long absorption cell fitted
with quartz windows. The instrument operates at a flow rate of 1.8 L min⁻¹. Wind speed and direction
were measured by an automated weather station installed on a ridge 900 m above the sampling site for
BC and O₃.

Formatted: Subscript

~~The observatory operated from January 2013 through July 2015. The observations used in this study cover January 2013 to August 2015, but periodic power disruptions caused occasional data gaps (Supplementary Table 1). Unless otherwise noted, data reported herein correspond to periods when BC, O₃ and meteorological data were available simultaneously. Measurements of carbon monoxide were suspended in late 2012 due to limited power supply. Unless otherwise noted, data reported herein correspond to periods when BC, O₃ and meteorological data were available simultaneously. Data are binned by season as follows: monsoon (July-September), post-monsoon (October-February) and pre-monsoon (March-June). Times correspond to Nepal's local time (LT) (UTC + 5.75 h). An automated weather station was installed on a ridge (3700 m) above the Jomsom observatory (JSM_1) and was operational from July 2012 to July 2015.~~

From March to May 2015, four additional automated weather stations were operated along a transect about 10 meters above and in the center of the valley floor where wind speeds are typically highest: near the entrance of the valley at Lete (LET), within the core at Marpha (MPH) and Jomsom (JSM_2), and near exit at Eklobhatti (EKL) (Fig. 1b). Power outages, instrument malfunction and a major earthquake in Nepal on April 25th, 2015 (and its aftershocks) limited the durations of record at all sites. However, between 1st and 14th May, all stations operated simultaneously and the resulting data provide information with which to evaluate diurnal variability of wind fields along the valley.

BC, O₃ and meteorological data were averaged over 10 minute intervals.

~~Power outages and instrument malfunction limited the durations of record at all sites. However, between 8th and 14th May, all stations operated simultaneously and the resulting data provide valuable information with which to evaluate diurnal variability of wind fields within the valley.~~

~~O₃, BC and meteorological data were averaged over 10 minute intervals. In order to characterize relative diurnal variability, O₃ and BC concentrations measured during a given month were normalized to a common scale ranging from 0 to 1 by subtracting the minimum for the month from each individual value and then dividing by the range for the month. The data were then binned into twenty-four, 1-hour increments and plotted.~~

3. Results and Discussion

3.1 Seasonal variability in BC and O₃

All data generated during the measurement period were binned by month to evaluate the seasonal patterns of BC and O₃ (Fig. 23). On addition, individual months with the most complete data coverage during the pre-monsoon (April 2013), monsoon (August 2014), and post-monsoon (November 2014) seasons were selected to evaluate aspects of temporal variability in more detail (Fig. 4). Based on

255 median values, the highest concentrations of both species were during the months preceding the
monsoon and the lowest were during months of the monsoon. We infer that the significantly lower
concentrations during the monsoon reflect the influences of synoptic easterly airflow that transports
cleaner marine air mass over the region, reduced agricultural residue burning (Sarangi et al., 2014), and
more efficient removal via wet deposition (Dumka et al., 2010). O₃ production is also suppressed under
260 cloudy conditions during the monsoon (Lawrence and Lelieveld, 2010). Median concentrations of both
species were systematically lower during monsoon months relative to the rest of the year. BC
concentrations during the monsoon period relative to non-monsoon period were lower. We infer that the
lower concentrations during the monsoon reflect the influences of reduced biomass burning and
associated emissions coupled with more efficient removal via wet deposition during the monsoon. The
265 highest median values and ranges for both species occurred during the pre-monsoon period.
Representative months from each season, April 2013 (pre-monsoon), July 2015 (monsoon) and
November 2014 (post-monsoon), were selected based on data availability and quality to evaluate
aspects of temporal variability in more detail. O₃ varies seasonally in the KGV, with highest mixing
ratios during the pre-monsoon season and lowest during the monsoon (Fig. 2 and 3). BC and O₃ in
270 monsoon is relatively smaller to those of non-monsoon months due in part to the southwesterly air flow
that brings cleaner marine air mass from the oceans and suppressed O₃ production under cloudy
conditions during the monsoon season (Lawrence and Lelieveld, 2010).

Similar seasonalSeasonal variability in BC concentration is evident across the IGP from urban to remote
locations and up in the Himalayan valleys like at the KGV indicating a broad regional pattern. The
275 seasonal peaks observed at KGV, a remote Himalayan valley, are consistent with patterns to stations
across the IGP. For example, high concentrations of BC (~1.48 to 1.99 $\mu\text{g m}^{-3}$) have been reported in
near-surface air across the IGP as well as in layers of the atmosphere at ~900 m asl and ~1200 m asl
during the post-monsoon over Northern India (Tripathi et al, 2005; 2007). Sreekanth et al (2007)
reported BC concentrations in Vishakhapatnam, in eastern India, at 8.01 $\mu\text{g m}^{-3}$ in pre-monsoon and 1.67
280 $\mu\text{g m}^{-3}$ during monsoon while Ramchandran et al (2007) observed BC concentrations in Ahmedabad,
western India, of 0.8 $\mu\text{g m}^{-3}$ during the monsoon in July to 5 $\mu\text{g m}^{-3}$ during the post monsoon in January,
and increased to 5 $\mu\text{g m}^{-3}$ during the post-monsoon in January (Ramchandran et al, 2007). Similar
seasonable variability has also been reported in the high Himalaya. For example, The the Nepal
285 Climate Observatory-Pyramid (NCO-P) station at the 5079 m asl in the Himalaya has also shown high
seasonal trends for BC (0.444 (\pm 0.443) $\mu\text{g m}^{-3}$ during pre-monsoon and 0.064 (\pm 0.101) $\mu\text{g m}^{-3}$ during
monsoon season and ozone concentrations 61 (\pm 9) ppbv during pre-monsoon season and 39 (\pm 10) ppbv
during monsoon (Cristofanelli et al., 2010, Marinoni et al., 2013) (Table 1).

Our results indicate that seasonable variability in BC and O₃ within the KGV and presumably other
deep Himalayan valleys is coupled with these larger regional-scale patterns.

290 These differences in sources, atmospheric chemistry and processing contribute to differential seasonal
(and diurnal) patterns in BC and O₃ in the KGV. BC in the Himalaya region is closely linked with

regional emissions from forest fires, agricultural burning, exhaust from diesel vehicles, gas-powered generator sets for power, power plants, and brick kilns over the IGP (Lawrence and Lelieveld, 2010).

3.2 Diurnal variability in BC and O₃

To normalize for the influence of day-to-day variability in absolute concentrations, relative diurnal variability in O₃ and BC concentrations measured during a given month were normalized to a common scale ranging from 0 to 1 by subtracting the minimum for the month from each individual value and then dividing by the range for the month (e.g., Sander et al., 2003; Fischer et al., 2006). The data were then binned into twenty-four, 1-hour increments and plotted (Fig. 5). Normalized diurnal cycles of O₃ and BC reveal several distinct patterns (Fig. 3). Based on median values during all three periods, O₃ peaked during daytime and dropped to minimal levels before sunrise. However, in the pre-monsoon period, O₃ peaked in the late afternoon whereas in the post-monsoon, it peaked in the early afternoon. In addition, the normalized diurnal excursions were greater during the pre- and post-monsoon periods relative to the monsoon period. Finally, the 10th through 90th percentiles of the concentration range accounted for most of the normalized scale from 0 to 1 (Fig. 3).

In contrast, based on median values during all three periods, BC concentrations increased rapidly following sunrise, decreased during late morning, and then rose through the afternoon and early evening hours (Fig. 3). Relative diurnal variability was somewhat greater during the post- relative to the pre-monsoon periods and lower during the monsoon period. The more skewed distributions for BC relative to O₃ reflect infrequent periods of high concentrations during all three seasons.

Notably, the 10th through 90th percentiles of the concentration range for most time intervals during the pre- and post monsoon periods fell within the lower half of the normalized range and those for the monsoon period fell within the lowest 10% of the normalized range. These skewed distributions reflect infrequent periods of relatively high BC concentrations during all three seasons.

Several factors contributed to differences in the diurnal variability of O₃ and BC. These include diurnal variability in emissions of BC versus O₃ precursors and/or production in source regions followed by regional transport, diurnal variability in the photochemical chemical production and destruction of O₃, and contributions of O₃ from non-combustion sources. O₃ is produced photochemically and is lost via deposition to surfaces and chemical reactions. O₃ is produced photochemically during daytime and is lost via deposition to surfaces and chemical reactions. Consequently, O₃ typically peaked in the afternoon and decreased over night (Figure 3). The reduced radiation associated with increased cloud cover during the monsoon likely contributed to the relatively lower diurnal variability during that period relative to the pre- and post monsoon periods.

In contrast, BC is a primary emission product of combustion that may originate from both local and distant sources. The early morning peak during all three seasons suggests probable

Formatted: Font: (Intl) Calibri

330 contributions from the local combustion of biofuels for cooking and heating, which are most prevalent during early morning. The secondary peak in the afternoon and early evening occur when the local anthropogenic sources are at minimum in the KGV. Up-valley air transports air mass from the plains via valley wind system analogous to “Alpine pumping”. As discussed in more detail below, the local wind fields within the KGV appear to have driven diurnal variability in BC.

3.3 Evolution of local wind system in the KGV

335 Measurements from JSM_2 show the diurnal evolution of wind in each season. All data collected were used to analyze the diurnal pattern of wind at Jomsom (Fig. 6). The wind roses illustrate the temporal evolution of up- and down-valley flows at JSM_2 for each season (Fig. 6). At JSM_2, up-valley flows are southwesterly and dominant during daytime with peak velocities above 15 m s^{-1} between about 0900 LT to 1800 LT. Wind velocities decreased substantially after 1800 LT, with variable wind direction until midnight then northeasterly winds are common during pre- and post-monsoon seasons (Fig. 6a and 6c)). The wind pattern during monsoon was strongly influenced by the monsoon anticyclone, this observation is in agreement with wind direction from other Himalayan valleys (Bonasoni et al., 2010; Ueno et al., 2008) (Fig. 6b) Although wind velocities at JSM_2 varied somewhat over the year, non-monsoon months exhibited similar diurnal patterns that evolved seasonally as a function of sunrise and sunset (Fig. 6) unlike in the monsoon season. As discussed below, this alternating pattern in wind direction from strong daytime flows to weak nighttime flows during dry months results in a net transport of pollutants up the valley.

340 Theodolite observations at different locations along the KGV in 1998 show minor shifts - less than 45° - in wind direction and less than 2 m s^{-1} in wind speed in the lower 1000 m above the surface during daytime (Egger et al 2000). Based on the average daytime wind speed, the valley can be partitioned into three regions: the entrance, core, and exit (average wind speeds range from 5 to 10 m s^{-1} , 8 to 18 m s^{-1} , and less than 5 m s^{-1} , respectively) (Egger et al 2000). The strongest winds within the core region are most prevalent in the lower 1000 to 1500 m of the boundary layer within the valley (Egger et al. 2000; Zängl et al., 2000, Egger et al., 2002). Our measurements at the four AWS stations on the valley floor illustrate the evolution of surface wind velocities along the length of the KGV (Supplementary Figure 1). In addition, comparison between measurements at JSM_1 between 1st and 14th May 2015 and the longer-term record JSM_2 for same period (Fig. 6 and Supplementary Figure 1) provide information regarding vertical variability. Velocities at the higher elevation site of JSM_2 were about 5 m s^{-1} greater than those near the valley floor during the day and 3 m s^{-1} stronger at nighttime but with similar diurnal cycles. While there is a relatively stronger northeasterly wind at JSM_2 from 0300 to 0900 LST in comparison to JSM_1. Airflow along the valley is driven by gradients in temperature and pressure between the entrance and the exit regions of the valley (Egger, 2000). Wind speed along the valley floor peaked within the core of the valley at MPH, JSM_1 and JSM_2 and were lower in the entrance (LET) and exit (EKL) regions (Supplementary Figure 1). The duration of strong wind speeds within the valley

365 during daytime is consistent with the hypothesis that wind patterns are modulated by the pressure
gradient created as a result of differential heating of the arid valley floor relative to the mouth of the
valley Egger et al. (2000).

370 Theodolite observations at different locations along the KGV in 1998 show minor shifts — less than 45°—
in wind direction and less than 2 m s⁻¹ in wind speed in the lower 1000 m above the surface during
daytime (Egger et al 2000). However at nighttime, deviation in wind speed and direction from daytime
conditions is expected due to strong nocturnal stratification. At approximately 900 m above the valley
floor, JSM2 is likely to be within the residual layer during nighttime. Measurements at the four AWS
stations on the valley floor illustrate the evolution of surface wind velocities at various locations within
the KGV (Fig. 4). Comparison between the short term record for 8 to 14 May 2015 at JSM2 (Fig. 4)
and the longer term record for the entire month May 2013 at JSM1 (Supplement) reveal that velocities
at the higher elevation site were about 5 m s⁻¹ greater than those near the valley floor but with similar
diurnal cycles. Although wind velocities at JSM2 varied somewhat over the year, all months exhibited
similar diurnal patterns that evolved seasonally as a function of sunrise and sunset (Supplement).

380 Air flow along the valley is driven by gradients in temperature and pressure between the entrance and
the exit regions of the valley. The windroses (Fig. 4a) illustrate the temporal evolution of up and down
valley flows along the valley floor. At Jomsom, up valley flows are southwesterly and dominant during
daytime with peak velocities of 10 to 15 m s⁻¹ between about 0900 LT to 1800 LT. The wind velocities
along the valley peaked within the core of the valley at MPH and JSM2 and were lower at the entrance
(LET) and exit (EKL) regions (Fig. 4b). The duration of strong wind speeds within the valley during
daytime supports the hypothesis that wind flow is modulated by the pressure gradient created as a result
of differential heating of the arid valley floor relative to the mouth of the valley. The finding is in
agreement with that of Egger et al. (2000) that the wind velocity is driven by the gradient in temperature
thus pressure between the entrance and the exit regions of the valley. Wind velocities decreased
substantially after 1800 LT, with variable wind direction possibly due to the influence of down slope
flows in the valley when the down valley flows were weak.

390 **3.4 Local wind drivers of BC and O₃ in the KGV**

395 Figure 6-4 shows the time series of BC and O₃ during individual months (April/pre-monsoon,
July/August/monsoon, November/post-monsoon) that are representative of each season. For pre-
monsoon, BC concentrations peaked at 0700 LST (Fig. 4) when wind velocities were low (Fig. 4). For
both pre-monsoon and monsoon periods, BC concentrations peaked at 0700 LST (Fig. 4) when wind
velocities were low (Fig. 5). This peak occurred about an hour later during the post monsoon period,
with all seasons experiencing decrease in BC over the rest of the morning as wind speeds increase (Fig.
45). Dilution of local emissions associated from increasing wind speed likely contributes to decreasing
BC concentration during late morning. Calm wind speed, higher use of biofuel burning for cooking and

400 ~~slowly decaying nocturnal boundary layer in the morning limit emission flow close to the source. Assuming that the early morning peak reflects contributions from local sources, decreasing concentrations with increasing wind speeds are consistent with expectations based on dilution.~~

Thereafter, concentrations increased over the afternoon and early night, reaching secondary peaks near midnight LST during the pre-monsoon and several hours earlier during other periods (Fig. 4 and 65).

405 ~~Distinct morning and afternoon peaks are seen in post-monsoon season when the up-valley wind speeds are relatively calmer than in pre-monsoon season (Fig. 5 and 6). Bimodal diurnal distribution of diurnal BC concentration in Jomsom is similar to that in high elevation sites where similar non-monsoonal diurnal peaks were observed (Bonasoni et al., 2010; Hindman et al., 2002; Hegde et al., 2007). The secondary peaks are the result of mountain-valley wind system pumping air from over the plains through the KGV.~~ Ozone exhibits a distinct minimum in the early morning. However, mixing ratios increase during the morning, peak in the early afternoon well before that of BC and decrease over night.

415 Percentage distributions of up-valley and down-valley BC concentrations, fluxes and net daily fluxes per unit cross section are depicted in Figure 7 and summarized in Supplementary Table 2. Up-valley (southwesterly) flows are defined as between 35° and 55° while down-valley (northeasterly) flows include data between 215° and 235°. Data for all days for which complete data were available over entire 24-hour periods were binned by season. The statistical significance of differences between up-valley and down-valley flow conditions during different seasons were evaluated using the non-parametric Kruskal Wallis and Mann-Whitney tests. The distribution of BC concentrations between up-valley and down-valley flow are statistically significant for all seasons (Figure 7a). However, because wind velocities were relatively higher during up-valley daytime flow and the durations of up-valley were modestly longer than those of down-valley flow, the corresponding up-valley fluxes of BC during daytime were significantly greater than down-valley fluxes during all seasons (Fig. 7b). These results suggest an oscillatory movement of polluted air within the valley. Differences between up-valley versus down-valley fluxes yielded significant net positive up-valley fluxes of BC during all seasons (Fig. 7c). Because heating would have driven growth of the boundary layer and thus greater ventilation and dilution of pollutants during daytime relative to night, we infer that the calculated differences in up-valley versus down-valley fluxes correspond to lower limits for net BC fluxes.

430 Positive up-valley fluxes are consistent with an “alpine pumping” mechanism in the Himalayan valleys and thereby support the hypothesis that these valleys are important pathways for pollution transport. If we assume that (1) the polluted boundary layer within the valley at Jomsom is 800 m deep (i.e., the approximate elevational difference between the two AWS sites at Jomsom), (2) BC within the polluted boundary layer is well mixed, and (3) wind velocities do not vary significantly with altitude through the polluted layer, the mass flux BC through a vertical plane across the valley can be estimated. Because some BC is almost certainly transported above 800 m elevation, this approach yields a conservative estimate. The long lifetime of particulate BC against deposition (several days to a week or more) coupled with turbulent flow within the valley supports the assumption that BC is well mixed. As noted previously, wind velocities measured at JSM 1 (2800 m) and JSM 2 (3700 m) were similar suggesting

440 minimal variability through the lower 800 m depth of the valley. Extrapolation of the net daily BC flux per unit area to the cross-sectional plane of the valley at Jomsom (1.62 km²) yields net daily fluxes of BC through the valley during the pre-monsoon season of 1.2 kg day⁻¹ (based on the average daily net flux) and 0.96 kg day⁻¹ (based on the median daily net daily flux). Such estimates provide useful semi-quantitative constraints on mass fluxes of BC from the IGP to the high Himalaya through deep valleys and, more generally, on the regional cycling of BC over southern Asia.

445 Interseasonal variability in the timing of the morning BC peak is likely related to seasonal changes in sunrise and corresponding temporal changes to thermal driven pressure gradients coupled with shifts in daily activities and associated emissions such as cooking and heating with biofuels. BC measurements at the JSM STA—on the east facing slope of the valley—suggest that strong upslope flows in the morning coincide with weaker down valley flow and higher local pollution from cooking. These strong upslope morning flows likely transport the local pollution upslope rather than up valley, while during the day after the boundary layer is fully developed strong up valley flows occur (Fig. 5). Dilution of local emissions associated from increasing wind speed likely contributes to decreasing BC concentration during late morning.

450 In addition to the wind pattern, the growth of the boundary layer also affects surface concentration. Nocturnal decoupling of the boundary layer preserves the concentration of both O₃ and BC in the valley from the previous day. A shallow morning boundary layer in conjunction with stronger upslope flows and emissions from biofuel burning increases surface concentrations of BC, while the strong wind speed along with the growing boundary layer strengthens the dilution effect in the valley. These diurnal patterns are occasionally replaced by periods of high BC or O₃ in the pre and post monsoon seasons.

460 **3.4 Evidence of transport episodes in valley concentration**

3.4.1 BC and O₃ concentration anomaly

465 Along with the regular diurnal and seasonal variability driven by local winds as described above, we also observed anomalous periods when for several days concentrations of both BC and O₃ were significantly greater than the 90th percentile for their corresponding monthly annual averages (Supplement Table 3). These extended periods of high BC and O₃ are possible evidence of large scale transport from the IGP ~~to the~~ to the foothills in conjunction with local valley winds (Fig. 8) TP via trans-Himalayan valleys.

470 We identified three common patterns in the BC profile at Jomsom during the transport episodes. For most of the transport episodes were associated with observational evidence from satellite imagery of emission sources within the region including haze over IGP, agricultural and biomass burning in Punjab regions of India and Pakistan, and forest fires in the foothills of the Himalaya in northern India or

southern Nepal (Supplement Table 3). The 90th percentile for each year 2013, 2014 and 2015 were 1.53 $\mu\text{g m}^{-3}$, 1.60 $\mu\text{g m}^{-3}$ and 1.47 $\mu\text{g m}^{-3}$ respectively. The year 2015 only included January through July data. We partition these episodes into three characteristic patterns based on relative variability. Pattern A was characterized as a fluctuating daily maxima in BC with peaks that repeatedly exceeded the 90th percentile but with daily relatively lower minima (Fig. 8[Ia]). Pattern B was characterized as regional transport periods when a buildup of BC concentration was seen over the period without a relatively low daily minima but peak concentrations over the 90th percentile (Figure 8b). While Pattern C corresponded to the periods when the BC concentration exhibited both pattern A and B during a single regional episode (Figure 8c). A total of 31 regional episodes were identified from January 2013 till July 2015, 50% of which were pattern A, 30% Pattern B and 20% pattern C. The wind speeds at Jomsom during these transport episodes exhibited diurnal variability similar to those during other periods (Fig. 8 [II]). We initiated the Hybrid Single-Particle Lagrangian Integrated Trajectory model (HYSPLIT), developed by NOAA's Air Resources Laboratory, from 300 m, 500 m and 1000 m for 72 hours runtime for each of the example episodes (Stein et al., 2015). HYSPLIT trajectories show that the transport of air mass from the above source regions during that period (Fig. 9).

During the regional transport period in November 2014 (Pattern A), average daily BC concentration was 1.29 $\mu\text{g m}^{-3}$ which is over the 75th percentile (0.88 $\mu\text{g m}^{-3}$) of the BC concentration for the measurement duration. The maximum daily concentration during the period was 3.04 $\mu\text{g m}^{-3}$. However, the corresponding average O₃ was only 28.07 ppbv, slightly below the average (29.48 ppbv) for the entire data set (Figure 8 [Ia]). The diurnal wind pattern in the KGV was conserved during pattern A (Figure 8 [IIa]). The MODIS fire data and HYSPLIT back trajectories showed extensive haze and fire events during this period of regional transport (Figure 9). We infer that transport of BC emitted from agricultural burning and wildfires during this period contributed to the high concentration measured with the KGV.

The mean BC concentration during pattern B, one example of which occurred in May 2014, was 1.77 $\mu\text{g m}^{-3}$ (Figure 8[IIb]). It was above the 90th percentile (1.49 $\mu\text{g m}^{-3}$) for entire measurement period while O₃ concentrations were at 49.71 ppbv, slightly below the 90th percentile (52.9 ppbv). The wind pattern in the KGV exhibited diurnal flow patterns but with longer period of up-valley flows compared to pattern A (Fig. 8 [IIb]). During this period MODIS imagery and HYSPLIT back trajectories revealed widespread burning in the Himalayan foothills and the Punjab region of India (Figure 9).

One of the Pattern C- type of transport episodes was identified in May 2013, when the average concentration was well above the 90th percentile for both BC (2.09 $\mu\text{g m}^{-3}$) and O₃ (57.49 ppbv) (Fig. 8 [IIc]). Diurnal wind patterns were similar to those of pattern B with extended duration of up-valley flows (Fig. 8 [IIc]). MODIS and HYSPLIT back trajectories revealed extensive agricultural burning in the Punjab region of India and the southern plains of Nepal during this period (Figure 9).

510 This assertion is reasonable because we assume that most pollution from local sources only occurs in the morning and is diluted by increased wind speed by mid-day. We identified three common patterns/transport episodes seen in the KGV (Figure 6).

515 During the regional transport episode in May 2013 (pattern A), average BC concentration ($2.45 \mu\text{g m}^{-3}$) was 102% higher than the 2-year average concentration, $1.21 \mu\text{g m}^{-3}$, for the month (Fig. 6). The corresponding O_3 concentration (58.37 ppbv) was 10% higher than the 2-year monthly average (53.26 ppbv). The MODIS fire data showed more than 100 fire events in the Punjab region of India for 5 out of 10 days during that period (Fig. 7a). The fire sources in Punjab during May 2013 is about 800 km away from Jomsom. The pollutants emitted from this crop residue burning increased BC concentration in the KGV valley from $0.8 \mu\text{g m}^{-3}$ to $2.08 \mu\text{g m}^{-3}$ as shown in figure 6. BC in the valley increased steadily from May 2nd until it reached over $4 \mu\text{g m}^{-3}$ on the 5th of May. This elevated concentration of BC persisted for 10 days.

520 The mean BC concentration during the regional transport episode in June (pattern B) was 125% higher than the average monthly mean for June ($1.01 \mu\text{g m}^{-3}$) while the mean O_3 mixing ratio (69.97 ppbv) exceeded the monthly mean (47.23 ppbv) by 45%. Again, during this time, MODIS fire imagery identified fires events in the foothills of the Himalaya in Western Nepal, about 300 km from KGV (Fig. 7b). However, though both patterns A and B appear to have resulted from extensive burning in the region, pattern B showed a slower rise in BC concentration in the valley and lasted for 5 days. The proximity to fire sources differentiated pattern A from pattern B.

525 Pattern C shows higher O_3 and BC concentrations as a result of extensive haze over IGP during Dec. 2014 (Fig. 6). The mean BC concentration during pattern C ($1.14 \mu\text{g m}^{-3}$) was 45% higher than the monthly average ($0.78 \mu\text{g m}^{-3}$) whereas O_3 mixing ratio decreased 10% from 33.19 ppbv monthly average to 30.02 ppbv. This suggests that the extensive haze during this period (Fig. 7c) attenuated incident solar radiation, thereby slowing the net photochemical production of O_3 .

530 The regional transport episodes highlighted above frequently occurred in the pre- and post-monsoon seasons when the synoptic winds are southwesterly, from the IGP, and wet deposition from precipitation is negligible. The local wind system of the Himalayan valleys is well-developed, and is the most important driving factor for the flow of air into the valleys. Emissions from crop residue burning and natural fires occur in the pre- and post-monsoon season, in addition to the regular, year-round emission sources like industries and vehicles. During agricultural crop residue burning, BC concentration peaks reached over $20 \mu\text{g m}^{-3}$ in Northern India (Khoral et al, 2012) which was similar to corresponding daily BC concentration peak observed in Kathmandu, Nepal (Putero et al, 2015).

540 Agricultural burning significantly contributes to high BC in the region during April-May and October-

545 ~~November, while forest fires are common in March–April. The MODIS fire product shows March through June as major fire season with about 2500 fire counts in the lower Himalaya, annually (Vadrevu et al., 2012). Lower temperatures in the winter season are responsible for more shallow boundary layers that confine the pollutants near the surface where they accumulate as a result of limited convection which results in the formation of haze in the region. All the above factors contribute to the elevated BC and O₃ concentration in the air, transported via the Himalayan valleys to higher elevations. Observations show that about 266 μg m⁻² of BC is deposited in the higher Himalaya during the pre-monsoon season, March–May (Yasunari et al., 2010).~~

550 **3.4.25 Pollution in the Higher Himalaya**

555 ~~Average BC concentrations in European cities like Barcelona, Lugano and London range between 1.7 to 1.9 μg m⁻³ (Reche et al., 2011). National Ambient Air Quality Standards (NAAQS) for the United States for O₃ is 70 ppbv (8-hour maximum average). During regional transport episodes, BC and O₃ levels in the remote site in Jomsom exceeded the above levels for both BC and O₃ occasionally. BC and O₃ concentrations suggest that the extensive haze layer over the IGP during pre-monsoon along with increased fire activity in the IGP and Himalayan foothills results in an increased flux of pollutants into the Himalayan valleys (Fig 6-7 and 78). The pollutants are transported by the local wind system, specifically the up valley winds that are dominant throughout the day. However, larger synoptic patterns are responsible for transport of pollutants from regional sources to the Himalayan foothills and the entrance region of valleys like the KGV.~~

560 ~~The results obtained at JSM STA show similar seasonal pattern as NCO-P CNR (Bonasoni et al., 2010) with higher concentration of BC and O₃ in the pre-monsoon season and lowest during the monsoon. However, the magnitude of concentration differ for both BC and O₃ at the two sites (Table 1). Our results from JSM STA found BC concentrations in the KGV are twice as high as those measured at NCO-P CNR during pre-monsoon season while O₃ concentration at NCO-P CNR were twice as high as JSM STA. At JSM STA during the post monsoon season, BC concentration are comparative to pre-monsoon season and 5 times higher than that at NCO-P CNR while O₃ concentrations remain higher at NCO-P CNR. The NCO-P CNR is at a higher elevation than Jomsom and can be affected by frequent stratospheric intrusions thus resulting in higher O₃ concentrations than that at Jomsom (Cristofanelli et al., 2010). Alternatively, BC is significantly higher in Jomsom for all seasons when compared to NCO-P CNR.~~

570 ~~Further analysis is needed to understand probable oscillation or stagnation of polluted air mass trapped in the valley as no dominant down valley flow was seen at nighttime in the valley floor except for at the entrance region, Lete. There is a strong possibility that the transported pollutants are stagnant at nighttime and are transported further up the valley when the nocturnal boundary layer dissolves and the strong up valley flow resumes. Stratospheric intrusions also influence the relative abundance of O₃ and~~

Formatted: Font: (Intl) Calibri

580 ~~BC in the high elevation Himalaya. Deep monsoon convection causes enhanced mass flux across the tropopause when the vertical temperature gradient is weak. This mass flux across the tropopause causes strong downdraft around the tropopause causing stratospheric exchange in mid latitudes (Kumar, 2006). Conditions for STE over the Himalaya is possible when the monsoon air masses move towards the Himalaya. Signatures of stratospheric intrusions have been observed at NCO-P during all seasons but predominantly during pre monsoon and post monsoon season (Bracci et al., 2011).~~

4. Conclusion

585 This study provides the ~~first~~ in-situ observational evidence of the role of trans-Himalayan valleys as ~~prominent important~~ pathways for ~~transporting~~ air pollutants ~~transport~~ from the IGP to the ~~TP~~ ~~higher~~ Himalaya.

We found that:

- ~~Concentrations of BC and O₃ in the KGV exhibited systematic diurnal and seasonal variability. The diurnal pattern of BC concentrations during the pre- and post-monsoon seasons were modulated by the pulsed nature of up-valley and down-valley flows. Seasonally, pre-monsoon BC concentrations of BC were higher than in post-monsoon season.~~
- ~~The morning and afternoon peaks in the post monsoon season was more pronounced than those of pre-monsoon season likely due to the relatively lower wind speeds during post-monsoon.~~
- ~~When compared to a high elevation site, NCO-P CNR in the Himalaya, JSM STA consistently showed higher BC concentrations for all seasons whereas the corresponding O₃ concentrations were higher at NCO-P CNR.~~
- ~~Significant positive up-valley fluxes of BC were measured during all seasons.~~
- ~~During episodes of regional pollution over the IGP, relatively higher concentrations of BC and O₃ were also measured in the KGV.~~
- ~~Further studies are needed to understand the vertical and horizontal distribution of particulate matter and ozone in the Himalayan region, and their impact on the radiative budget, the ASM and climate. Investigations using sondes, LiDar and air-borne measurements could help characterize the stratification of the vertical air masses.~~

605 ~~The concentrations of BC and O₃ in the KGV exhibited systematic diurnal and seasonal variability. During the non monsoon months, we observed episodes of high pollutant transport through the KGV. Our results suggest that transport through trans Himalayan valleys during episodic periods of regional~~

Formatted: Font: Times New Roman, 12 pt, Font color: Black, Text 1

Formatted: List Paragraph, Bulleted + Level: 1 + Aligned at: 0.25" + Indent at: 0.5"

Formatted: Font: Times New Roman, 12 pt, Font color: Black, Text 1

Formatted: List Paragraph, Bulleted + Level: 1 + Aligned at: 0.25" + Indent at: 0.5"

610 ~~pollution over the IGP accounts for disproportionately large fractions of total BC transport from southern Asia to the Tibetan Plateau.~~

615 ~~Further studies should be conducted to understand the vertical and horizontal distribution of particulate matter and ozone in the Himalayan region. Further investigation particularly using sondes and LiDAR could help understand the stratification of the vertical air masses. Our findings here can enhance the predictive capabilities of the scientific communities in analyzing the impacts of increasing air pollution in the Himalayan region, on human health, food security, economics, and available natural resources along with estimating the flux of pollutants through the Himalayan valleys.~~

Acknowledgments

620 We would like to acknowledge our field assistant in Nepal, Buddhi Lamichhane who helped us in various stages of the study, as well as the logistic and administrative support and internet at the Jomsom station provided by Nepal Wireless. Financial support was provided by the National Aeronautics and Space Administration NNX12AC60G, and additional field support was provided by ICIMOD's Atmosphere Initiative. The authors are very thankful for comments from William Keene and Jennie Moody.

References

630 Andreae, M. O. and Crutzen, P. J.: Atmospheric Aerosols: Biogeochemical Sources and Role in Atmospheric Chemistry, *Science*, 1052-1058, 1997.

Auffhammer, M., Ramanathan, V. and Vincent, J. R.: Integrated model shows that atmospheric brown clouds and greenhouse gases have reduced rice harvests in India, *PNAS* 10.1073/pnas.0609584104, 2006.

635 ~~Bracci, A., Cristofanelli, P., Sprenger, M., Bonafe, U., Calzolari, F., Duchi, R., Laj, P., Marinoni, A., Roccatto, F., Vuilleumoz, E., Bonasoni, P.: Transport of Stratospheric Air Masses to the Nepal Climate Observatory Pyramid (Himalaya; 5079 m MSL): A Synoptic Scale Investigation, *J Appl. Meteorol. Clim.*, 51,1489-1507, 2013.~~

640 Brun, J., Shrestha, P., Barros, A., P.: Mapping aerosol intrusion in Himalayan valleys using the Moderate Resolution Imaging Spectroradiometer (MODIS) and Cloud Aerosol Lidar and Infrared Pathfinder Satellite Observation (CALIPSO), *Atmos. Env.*, 45 (2011) 6382-6392, 2011.

645 Bonasoni, P., Laj, P., Marinoni, A., Sprenger, M., Angelini, F., Arduini, J., Bonafe, U., Calzolari, F., Colombo, T., Decesari, S., Di Biagio, C., di Sarra, A. G., Evangelisti, F., Duchi, R., Facchini, M. C., Fuzzi, S., Gobbi, G. P., Maione, M., Panday, A., Roccatò, F., Sellegri, K., Venzac, H., Verza, G. P., Villani, P., Vuillermoz, E., and Cristofanelli, P.: Atmospheric Brown Clouds in the Himalayas: first two years of continuous observations at the Nepal Climate Observatory-Pyramid (5079 m), *Atmos. Chem. Phys.*, 10, 7515–7531, doi:10.5194/acp-10-7515-2010, 2010.

650 Bond, T., Doherty, S., Fahey, D., Forster, P., Berntsen, T., DeAngelo, B., Flanner, M., Ghan, S., Kärcher, B., and Koch, D.: Bounding the role of black carbon in the climate system: A scientific assessment, *J. Geophys. Res.-Atmos.*, 118, 5380–5552, doi:10.1002/jgrd.50171, 2013.

655 Brun, J., Shrestha, P., Barros, A. P.: Mapping aerosol intrusion in Himalayan valleys using the Moderate Resolution Imaging Spectroradiometer (MODIS) and Cloud Aerosol Lidar and Infrared Pathfinder Satellite Observation (CALIPSO), *Atmos. Env.*, 45 (2011) 6382-6392, 2011.

660 Cristofanelli, P., Bracci, A., Sprenger, M., Marinoni, A., Bonafè, U., Calzolari, F., Duchi, R., Laj, P., Pichon, J. M., Roccatò, F., Venzac, H., Vuillermoz, E., and Bonasoni, P.: Tropospheric ozone variations at the Nepal Climate Observatory Pyramid (Himalayas, 5079 m a.s.l.) and influence of deep stratospheric intrusion events, *Atmos. Chem. Phys.*, 10, 6537–6549, doi:10.5194/acp-10-6537-2010, 2010.

665 Dey, S., and Di Girolamo, L.: A climatology of aerosol optical and microphysical properties over the Indian subcontinent from 9 yr (2000–2008) of Multiangle Imaging Spectroradiometer (MISR) data, *J. Geophys. Res.*, 115, D15204, doi:10.1029/2009JD013395, 2010.

670 Decesari, S., Facchini, M.C., Carbone, C., Giulianelli, L., Rinaldi, M., Finessi, E., Fuzzi, S., Marinoni, A., Cristofanelli, P., Duchi, R., Bonasoni, P., Vuillermoz, E., Cozic, J., Jaffrezo, J., L., Laj, P.: Chemical composition of PM₁₀ and PM₁ at the high-altitude Himalayan station Nepal Climate Observatory-Pyramid (NCO-P) (5079 m a.s.l.), *Atmos. Chem. Phys.*, 10: 4583–4596, 2010.

675 Bonasoni, P., Cristofanelli, P., Marinoni, A., Vuillermoz, E.: Atmospheric Pollution in the Hindu Kush–Himalaya Region. *Mountain Research and Development*, 32(4), 468–479. <http://doi.org/10.1659/MRD-JOURNAL-D-12-00066.1>, 2012.

680 DOTM-Vehicle data zonal wise till 2072 baishakh, Government of Nepal, Department of Transportation Management (<http://www.dotm.gov.np/uploads/files/Vehicle-data-zonal-wise-till-2072-baishakh.pdf>) accessed March 26th, 2016.

685 Dumka, U., C., Krishna Moorthy, K., Satheesh, S., K., Sagar, R., Pant, P.: Short-period modulations in aerosol optical depths over the central Himalayas: role of mesoscale processes, *J. Appl. Meteor. Climatol.*, doi: 10.1175/2007JAMC1638.1, 2008.

675 Dumka, U. C., Moorthy, K., Kumar, R., Hegde, P., Sagar, R., Pant, P., Singh, N., Babu, S.:
Characteristics of aerosol black carbon mass concentration over the high altitude location in the
central Himalayas from multi-year observations. *Atmos. Res.*, 96, 510-521 2010.

Egger, J., Bajracharya, S., Egger, U., Heinrich, R., Reuder, J., Shakya, P., Wendt, H., and Wirth, V.:
Diurnal winds in the Himalayan Kali Gandaki valley. Part I: observations, *Mon. Weather Rev.*, 128,
680 1106-1122, 2000.

Egger, J., Bajracharya, S., Egger, U., Heinrich, R., Kolb, P., Lammlein, S., Mech, M., Reuder, J.,
Schaper, W., Shakya, P., Schween, J. and Wendt, H.: Diurnal winds in the Himalayan Kali Gandaki
valley. Part III:remotely piloted aircraft soundings, *Mon. Weather Rev.*, **130**, 2042-2058, 2002.

Engling, G., and Galencser, A.: Atmospheric brown clouds: from local air pollution to climate change,
685 *Elements*, 6, 223-228, 2010.

Fadnavis, S., Semeniuk, K., Pozzoli, L., Schultz, M. G., Ghude, S. D., Das, S., and Kakatkar, R.:
Transport of aerosols into the UTLS and their impact on the Asian monsoon region as seen in a global
model simulation, *Atmos. Chem. Phys.*, 13, 8771–8786, 2013.

690 Fischer, E., Pszenny, A., Keene, W., Maben, J., Smith, A., Stohl, A., Talbot R.: Nitric acid phase
partitioning and cycling in the New England coastal atmosphere, *J. Geophys. Res.*, 111, D23S09,
doi:10.1029/2006JD007328, 2006.

Flanner, M. G., Zender, C. S., Hess, P. G., Mahowald, N. M., Painter, T. H., Ramanathan, V., Rasch,
P. J.: Springtime warming and reduced snow cover from carbonaceous particles, *Atmos. Chem.*
Phys., 9 (7), 2481- 2497, doi: 10.5194/acp-9-2481-2009, 2009.

695 Gautam, R., Hsu, N. C., Tsay, S. C., Lau, K. M., Holben, B., Bell, S., Smirnov, A., Li, C., Hansell, R.,
Ji, Q., S. Payra, S., Aryal, D., Kayastha, R., K. M. Kim, K. M. : Accumulation of aerosols over the
Indo-Gangetic plains and southern slopes of the Himalayas: distribution, properties and radiative
effects during the 2009 pre-monsoon season, *Atmos. Chem. Phys.*, 11, 12841–12863, 2011.

Gustafsson, O., Kruså, M., Zencak, Z., Sheesley, R., J., Granat, L., Engström, E., Praveen, P., S., Rao,
700 P., S., P., Leck, C., Rodhe, H.: Brown Clouds over South Asia: Biomass or Fossil Fuel Combustion?,
Science, 323, 495-498, 2009.

Hegde P., Pant, P., Naja, M., Dumka, U. C., and Sagar, R.: South Asian dust episode in June 2006:
Aerosol observations in the central Himalayas, *Geophys. Res. Lett.*, 34, L23802,
doi:10.1029/2007GL030692, 2007.

705 Henne, S., Furger, M., Nyeki, S., Steinbacher, M., Neininger, B., de Wekker, S.F.J, Dommen, J.,
Spichtinger, N., A. Stohl, A. and Prevôt A. S. H.: Quantification of topographic venting of

Formatted: Body, Indent: Left: 0", Hanging: 0.25"

Formatted: Font: Font color: Text 1

boundary layer air to the free troposphere, *Atmos. Chem. Phys.*, 4, 497–509, 2004.

Hindman, E. E. and Upadhyay, B. P.: Air pollution transport in the Himalayas of Nepal and Tibet during the 1995–1996 dry season, *Atmos. Environ.*, 36, 727–739, 2002.

710 Hyvärinen, A., P., Lihavainen, H., Komppula, M., Sharma, V., P., Kerminen, V., M., Panwar, T., S., Viisanen, Y.: Continuous measurements of optical properties of atmospheric aerosols in Mukteshwar, Northern India, *J. Geophys. Res.*, 114: D08207, doi: 10.1029/2008JD011489, 2009.

715 Hyvärinen, A., -P., Vakkari, V., Laakso, L., R. K. Hooda, R., K., Sharma, V., P., Panwar, T., S., Beukes, J., P., van Zyl, P., G., M. Josipovic, M., Garland, R. M., Andreae, M. O., Poschl, U., Petzold, A.: Correction for a measurement artifact of the Multi-Angle Absorption Photometer (MAAP) at high black carbon mass concentration levels, *Atmos. Meas. Tech.*, 6, 81–90, 2013

Jacobson, M., Z.: Strong radiative heating due to the mixing state of black carbon in atmospheric aerosols, *Nature*, 409, 695–697, 2001.

720 Janssen, Nicole A. H., Hoek, G., Simic-Lawson, M., Fischer, P., van Bree, L., Brink, H., Keuken, M., Atkinson, R. W., Anderson, H. R., Brunekreef, B., and Cassee, F. R.: Black carbon as an additional indicator of the adverse health effects of airborne particles compared with PM₁₀ and PM_{2.5}, *Environ. health persp.* 119 (12), 1691–1698, 2011.

725 Kang, S., Xu, Y., You, Q., Flugel, W-A., Pepin, N. and Yao, T. review of Climate and cryospheric change in the Tibetan Plateau, *Environ. Res. Lett.* 5(1), 015101, 2010.

Kaufman, Y. J., Tanré, D., and Boucher, O.: A satellite view of aerosols in the climate system, *Nature*, 419, 215–223, 2002.

730 Koch, D., Schulz, M., Kinne, S., McNaughton, C., Spackman, J.R., Balkanski, Y., Bauer, S., Bernsten, T., Bond, T.C., Boucher, O., Chin, M., Clarke, A., De Luca, N., Dentener, F., Diehl, T., Dubovik, O., Easter, R., Färe, D.W., Feichter, J., Fillmore, D., Freitag, S., Ghan, S., Ginoux, P., Gong, S., Horowitz, L., Iversen, T., Kirkevåg, A., Klimont, Z., Kondo, Y., Krol, M., Liu, X., Miller, R., Montanaro, V., Moteki, N., Myhre, G., Penner, J.E., Perlwitz, J., Pitari, G., Reddy, S., Sahu, L., Sakamoto, H., Schuster, G., Schwarz, J.P., Seland Ø, Stier P., Takegawa, N., Takemura, T., Textor, C., van Aardenne, J.A., Zhao, Y.: Evaluation of black carbon estimations in global aerosol models. *Atmospheric Chemistry and Physics* 9, 9001e9026. Komppula, M., Lihavainen, H., A.-P. Hyvärinen, A., -P., Kerminen, V., -M., Panwar, T., S., Sharma, V., P., Viisanen, Y.: Physical properties of aerosol particles at a Himalayan background site in India, *J. Geophys. Res.*, 112, doi:10.1029/2008JD011007, 2009.

740 Kharola, S., K., Badarinath, K., V., S., Sharma, A., R., Mahalakshmi, D. V., Singh, D., Prasad, V. K.: Black carbon aerosol variations over Patiala city, Punjab, India—A study during agriculture crop

~~residue burning period using ground measurements and satellite data, *J. Atmos. Sol. Terr. Phys.*, 84-85, 45-51, 2012.~~

745 Kopacz, M., Mauzerall, D., L., Wang, J., Leibensperger, E., M., Henze, D., K., and K. Singh, K.: Origin and radiative forcing of black carbon transported to the Himalayas and Tibetan Plateau, *Atmos. Chem. Phys.*, 11, 2837–2852, 2011.

Krupnick, A., J., Harrington, W., Ostro, B.: Ambient ozone and acute health effects: Evidence from daily data, *J. Environ. Econ. Manag.*, 18(1), 1-18, 1990.

~~Kumar, K. K., 2006: VHF radar observations of convectively generated gravity waves: Some new insights, *Geophys. Res. Lett.*, 33, L01815, doi:10.1029/2005GL024109.~~

750 Lau, K., M., Kim, M., K., Kim, K., M.: Asian summer monsoon anomalies induced by aerosol direct forcing: The role of the Tibetan Plateau, *Climate Dynamics*, 26, 855–864, 2006.

Lawrence, M. G. and Lelieveld, J.: Atmospheric pollutant outflow from southern Asia: a review, *Atmos. Chem. Phys.*, 10, 11017–11096, doi:10.5194/acp-10-11017-2010, 2010.

755 Lee K, Soon DH, Shugui H, Sungmin, Xiang Q, Jaiwen R, Yapping L, Rosmann KJRR, Barbante C, Bourton CF.: Atmospheric pollution of trace elements in the remote high-altitude atmosphere in Central Asia as recorded in snow from Mt Qomolangma (Everest) of the Himalayas, *Sci. Tot. Environ.* 404, 171-181, 2008.

Lu, Z., Zhang, Q., and Streets, D., G.: Sulfur dioxide and primary carbonaceous aerosol emissions in China and India, 1996–2010, *Atmos. Chem. Phys.*, 11, 9839-9864, 2011.

760 Luthi, Z., L., Skerlak, B., Kim, S., W., Lauer, A., Mues, A., Rupakheti, M., and Kang, S.: Atmospheric brown clouds reach the Tibetan Plateau by crossing the Himalayas, *Atmos. Chem. Phys.*, 15, 11, 6007-6021, 2015.

765 Ma, J., Chen, Y., Wang, W., Yan, P., Liu, H., Yang, S., Hu, Z., and Lelieveld, J.: Strong air pollution causes widespread haze-clouds over China, *J. Geophys. Res.*, 115, D18204, 2010.

Marinoni, A., Cristofanelli, P., Laj, P., Duchi, R., Calzolari, F., Decesari, S., Sellegri, K., Vuillermoz, E., Verza, P., Villani, P., Bonasoni, P. Aerosol mass and black carbon concentrations, a two year record at NCO-P (5079 m, Southern Himalayas), *Atmos. Chem. Phys.*, 10, 8551-8562, 2010.

770 Marinoni, A., Cristofanelli, P., Laj, P., Duchi, Putero, D., Calzolari, F., Landi, T., C., Vuillermoz, E., Maione, M., Bonasoni, P.: High black carbon and ozone concentrations during pollution transport in the Himalayas: Five years of continuous observations at NCO-P global GAW station, *J. Environ. Sci.*, 25(8) 1618–1625, 2013.

Formatted: Space After: 0 pt, Line spacing: At least 15.55 pt, Pattern: Clear (White)

775 Menon, S., Hansen, J., Nazarenko, L. and Yunfeng, L.: Climate Effects of Black Carbon Aerosols in Aerosols in China and India, *Science*, 297, 2250-2253, 2002.

Pant, P., Hegde, P., Dumka, U., C., Sagar, R., Satheesh, S., K., Krishna Moorthy, K., Saha, A., Srivastava, M., K.: Aerosol characteristics at high-altitude location in central Himalayas: optical properties and radiative forcing, *J. Geophys. Res.*, doi:10.1029/2005JD006768, 2006.

Formatted: Body, Indent: Left: 0", Hanging: 0.25"

Formatted: Font: Font color: Text 1

780 Piketh, S. J., Annegarn, H., J., and Tyson, P., D.: Lower tropospheric aerosol loadings over South Africa: The relative contribution of aeolian dust, industrial emissions, and biomass burning, *J. Geophys. Res.*, 104(D1), 1597–1607, 1999.

Putero, D., Cristofanelli, P., Marinoni, A., Adhikary, B., Duchi, R., Shrestha, S. D., Verza, G. P., Landi, T. C., Calzolari, F., Busetto, M., Agrillo, G., Biancofiore, F., Carlo, P. Di., Panday, A. K., Rupakheti, M., and Bonasoni, P.: Seasonal variation of ozone and black carbon observed at Pokhara, an urban site in the Kathmandu Valley, Nepal, *Atmos. Chem. Phys.*, 15, 13957–13971, 2015.

Qian, Y., Flanner, M. G., Leung, L. R., and Wang, W.: Sensitivity studies on the impacts of Tibetan Plateau snowpack pollution on the Asian hydrological cycle and monsoon climate, *Atmos. Chem. Phys.*, 11, 1929–1948, doi:10.5194/acp-11-1929-2011, 2011.

790 Raatikainen, T., Hyvärinen, A.-P., Hatakka, J., Panwar, T., S., Hooda, R., K., Sharma, V., P., Lihavainen, H.: The effect of boundary layer dynamics on aerosol properties at the Indo-Gangetic plains and at the foothills of the Himalayas, *Atmos. Env.*, 89, 548-555, 2014.

Raatikainen, T., Brus, D., Hooda, R., K., Hyvärinen, A.-P., Asmi, E., Sharma, V., P., Arola, A., Lihavainen, H.: Size-selected black carbon mass distributions and mixing state in polluted and clean environments of northern India, *Atmos. Chem. Phys.* 17, 371-383, 2017.

795 Ram, K., Sarin, M., M. and Hegde, P.: Long-term record of aerosol optical properties and chemical composition from a high-altitude site (Manora Peak) in central Himalaya, *Atmos. Chem. Phys.*, 10: 11791–11803, 2010.

Formatted: Body, Indent: Left: 0", Hanging: 0.25"

Formatted: Font: 12 pt, Font color: Text 1, Pattern: C

800 Ramanathan, V., and Carmichael, G.: Global and regional climate changes due to black carbon, *Nat. Geosci.*, 1(4), 221–227, 2008.

Ramanathan, V., Chung, C., Kim, D., Bettge, T., Buja, L., Kiehl, J., T., Washington, W., M., Fu, Q., Sikka, D., R., and Wild, M.: Atmospheric brown clouds: Impacts on South Asian climate and hydrological cycle, *PNAS*, 102(15), 5326-5333, 2005.

805 Ramanathan, V. and Crutzen, P. J.: New Directions: Atmospheric Brown “Clouds”, *Atmos. Env.*, 37, 4033-4035, 2003.

810 Ramachandran, S., Rajesh, T., A.: Black carbon aerosol mass concentrations over Ahmedabad, an urban location in western India: Comparison with urban sites in Asia, Europe, Canada, and the United States, *J Geophys. Res Atmos.* 112(D06211), doi/10.1029/2006JD007488, 2007.

Ramanathan, V., Ramana, V., M., Roberts, G., Kim, D., Corrigan, C., Chung, C., Winker, D.: Warming trends in Asia amplified by brown cloud solar absorption, *Nature*, 448(2), 575-578, 2007a.

815 Ramanathan, V., Li, F., Ramana, M.V., Praveen, P.S., Kim, D., Corrigan, C.E., Nguyen, H., Stone, E.A., Schauer, J.J., Carmichael, G.R., Adhikary, B., Yoon, S.C.: Atmospheric Brown Clouds: Hemispherical and Regional Variations in Long-Range Transport, Absorption, and Radiative Forcing, *J. Geophys. Res.*, 112, D22821, 2007b.

820 Reche, C., Querol, X., Alastuey, A., Viana, M., Pey, J., Moreno, T., Rodríguez, S., González, Y., Fernández-Camacho, R., De La Campa, A. M, Sálnchez, De La Rosa, J., Dall'Osto, M., Prévôt, A. S H, Hueglin, C., Harrison, R. M., Quincey, P.: New considerations for PM, Black Carbon and particle number concentration for air quality monitoring across different European cities, *Atmos. Chem. Phys.*, 11, 6207–6227, 2011.

825 Reddy, M.S. and Venkataraman, C.: Inventory of Aerosol and Sulphur Dioxide Emissions from India: II – Biomass Combustion, *Atmos. Envir.*, 36 (4), 699-712, 2002.

Reiter, E. R., and Tang, M.: Plateau effects on diurnal circulation patterns. *Mon. Wea. Rev.*, 112, 638–651, 1984.

830 Sander, R., Keene, W. C., Pszenny, A. A. P., Arimoto, R., Ayers, G. P., Baboukas, V., Chaine, J. M., Crutzen, P. J., Duce, R. A., Hönninger, G., Huebert, B. J., Maenhaut, W., Mihalopoulos, N., Turekian, V. C., van Dingenen, R.: Inorganic bromine in the marine boundary layer: A critical review, *Atmos. Chem. Phys.* 3, 1301-1336, 2003.

Sarangi, T., Naja, M., Ohja, N., Kumar, R., Lal, S., Venkataramani, S., Kumar, A., Sagar, R., Chandola, H., C.: First simultaneous measurements of ozone, CO and NO_y at a high-altitude regional representative site in the central Himalayas, *JGR*, 119(3), 1592-1611, 2014).

835 Singh R. P., Dey, S., Tripathi, S. N., Tare, V., and Holben, B.: Variability of aerosol parameters over Kanpur, northern India, *J. Geophys. Res.*, 109, D23206, doi:10.1029/2004JD004966, 2004.

Sreekanth, V., Niranjan, K., Madhavan, B. L.: Radiative forcing of Black Carbon over Eastern India, *Geophys. Res. Lett.*, 34(L17818), doi: 10.1029/2007GL030377, 2007.

840 Srivastava, A., K., Singh, S., Pant, P. and Dumka, U., C. : Characteristics of black carbon over Delhi and Manora peak - A comparative study, *Atmos. Sci. Lett.*, 13: 223–230, 2012.

Stein, A.F., Draxler, R.R., Rolph, G.D., Stunder, B.J.B., Cohen, M.D., and Ngan, F., (2015). NOAA's HYSPLIT atmospheric transport and dispersion modeling system, *Bull. Amer. Meteor. Soc.*, 96,

Formatted: Body, Indent: Left: 0", Hanging: 0.25"

Formatted: Font color: Text 1

Formatted: Body, Indent: Left: 0", Hanging: 0.25"

Formatted: Font: Font color: Text 1

Formatted: Body, Indent: Left: 0", Hanging: 0.25"

2059-2077, <http://dx.doi.org/10.1175/BAMS-D-14-00110.1>, 2015.

Formatted: Font: Font color: Text 1

Steinacker, R.: Area–height distribution of a valley and its relation to the valley wind, *Beitr. Phys. Atmos.*, 57, 64–71, 1984.

Streets, D. G., Bond, T. C., Carmichael, G. R., Fernandes, S. D., Fu, Q., He, D., Klimont, Z., Nelson, S. M., Tsai, N. Y., Wang, M. Q., Woo, J. H., and Yarber, K. F.: An inventory of gaseous and primary aerosol emissions in Asia in the year 2000, *J. Geophys. Res.-Atmos.*, 108, 8809, doi:10.1029/2002JD003093, 2003.

The Royal Society, 2008. Ground-level ozone in the 21st century: future trends, impacts and policy implications. Science policy report 15/08. The Royal Society, London.

Tripathi, S. N., Dey, S., Tare, V., Satheesh, S. K.: Aerosol black carbon radiative forcing at an industrial city in northern India. *Geophys. Res. Lett.* 32 (L08802). doi:10.1029/2005GL022515, 2005.

Tripathi, S. N., Srivastava, A. K., Dey, S., Satheesh, S. K., Moorthy, K. K.: The vertical profile of atmospheric heating rate of black carbon aerosols at Kanpur in northern India. *Atmos. Env.* 41: 6909–6915, 2007.

Ueno, K., Toyotsu, K., Bertolani, L., and Tartari, G.: Stepwise onset of Monsoon Weather Observed in the Nepal Himalayas, *Mon. Weather Rev.*, 136(7), 2507–2522, 2008.

Formatted: Body, Indent: Left: 0", Hanging: 0.25"

Vasilyev, O. B., Contreras, A. L., Velazquez, A. M., Fabi, R., P., Ivlev, L., S., Kovalenko, A., P., Vasilyev, A., V., Jukov, V., M., and Welch, R., M.: Spectral optical properties of the polluted atmosphere of Mexico City (spring-summer 1992), *J. Geophys. Res.*, 100(D12), 26027–26044, 1995.

Formatted: Font color: Text 1

~~Whiteman, C. D., and Bian X.: Use of radar profiler data to investigate large-scale thermally driven flows into the Rocky Mountains, *Proc. Fourth Int. Symp. on Tropospheric Profiling: Needs and Technologies*, Snowmass, CO, 1998.~~

Formatted: Body, Indent: Left: 0", First line: 0"

Weissmann, M., Braun, A. F. J., Gantner, A., L., Mayr, A., G., J., Rahm, A., S., Reitebuch, A., O. :The Alpine Mountain–Plain Circulation: Airborne Doppler Lidar Measurements and Numerical Simulations, *Mon. Weather Rev.*, 133,(11), 3095-3109, 2005.

Whiteman, C. D., and Bian X.: Use of radar profiler data to investigate large-scale thermally driven flows into the Rocky Mountains, *Proc. Fourth Int. Symp. on Tropospheric Profiling: Needs and Technologies*, Snowmass, CO, 1998.

Vadrevu, K., P., E., K., V., S., Vermote, E.: MODIS derived fire characteristics and aerosol optical depth variations during the agricultural residue burning season, north India, *Environ. Pollut.*, 159(6), 1560–1569, 2011.

~~Vasilyev, O. B., Contreras, A., L., Velazquez, A., M., Fabi, R., P., Ivlev, L., S., Kovalenko, A., P., Vasilyev, A., V., Jukov, V., M., and Welch, R., M.: Spectral optical properties of the polluted atmosphere of Mexico City (spring-summer 1992), *J. Geophys. Res.*, 100(D12), 26027–26044, 1995.~~
880 Xu, C., Ma, Y. M., You, C., and Zhu, Z. K.: The regional distribution characteristics of aerosol optical depth over the Tibetan Plateau, *Atmos. Chem. Phys.*, 15, 12065–12078, 2015.

Yasunari, T. J., Bonasoni, P., Laj, P., Fujita, K., Vuillermoz, E., Marinoni, A., Cristofanelli, P., Duchi, R., Tartari, G., and Lau, K., M.: Estimated impact of black carbon deposition during pre-monsoon season from Nepal Climate Observatory - Pyramid data and snow albedo changes over Himalayan glaciers, *Atmos. Chem. Phys.*, 10(6), 603–6,615, 2010.

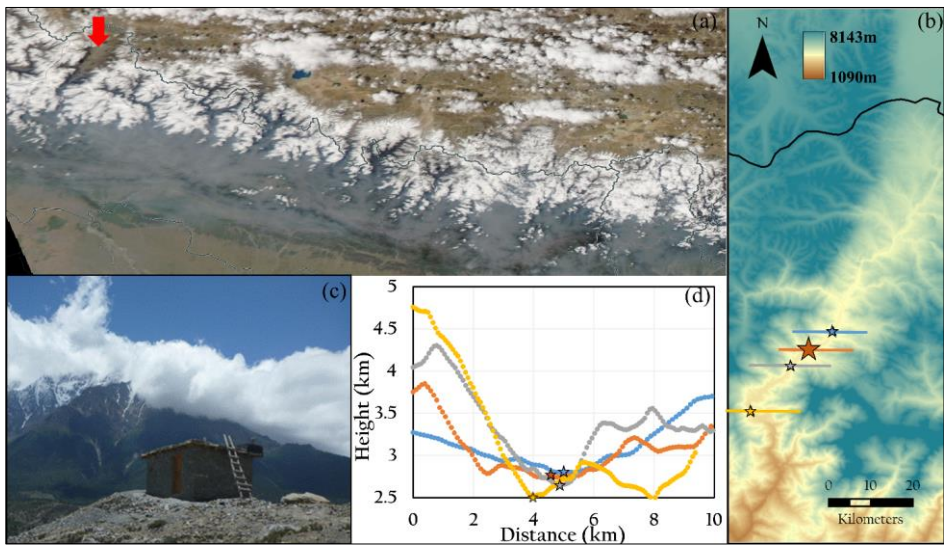
~~Wang, X. and Mauzerall, D. L.: Characterizing distributions of surface ozone and its impact on grain production in China, Japan and South Korea: 1990 and 2020, *Atmos. Environ.* 38, 4383–4402, 2004.~~

~~Xu, C., Ma, Y. M., You, C., and Zhu, Z. K.: The regional distribution characteristics of aerosol optical depth over the Tibetan Plateau, *Atmos. Chem. Phys.*, 15, 12065–12078, 2015.~~

890 Zangl, G., Egger, J., and Wirth, V.: Diurnal Winds in the Himalayan Kali Gandaki Valley. Part II: Modeling, *Mon. Weather Rev.*, 129, 1062–1080, 2000.

Formatted: Space After: 8 pt, Line spacing: Multiple 1.08 li, Adjust space between Latin and Asian text, Adjust space between Asian text and numbers

Commented [SD1]: Figure 1 is updated.



(UPDATED) Figure 1. (a) NASA Worldview image from November 4th, 2014 depicting thick haze intruding the Himalayan foothills with red arrow over the KGV. (b) Expanded scale of the KGV showing locations of LET near the entrance of the valley (yellow star); MPH in the core region (gray star); the JSM_STA sampling station for BC and O₃ and the two associated AWS sites (JSM_1 and JSM_2) in the core region (orange star); and EKL near the exit (blue star). (c) The atmospheric observatory at Jomsom (JSM_STA). (d) Cross-sectional elevation profile at the indicated locations.

905

910

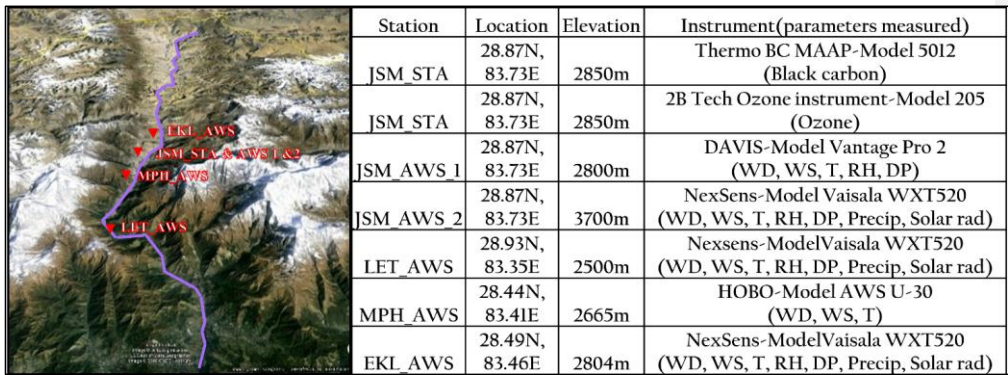
915

920

925

930

935



(UPDATED)Figure 2. The valley floor of KGV is shown in purple along with details

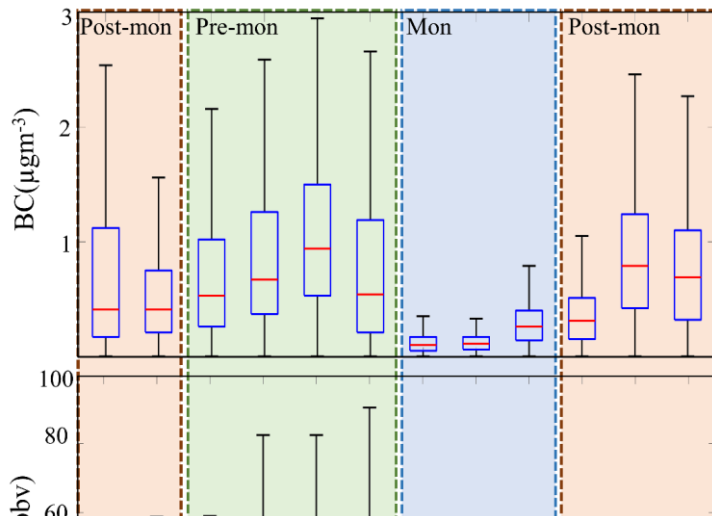
940

945

950

955

960



965

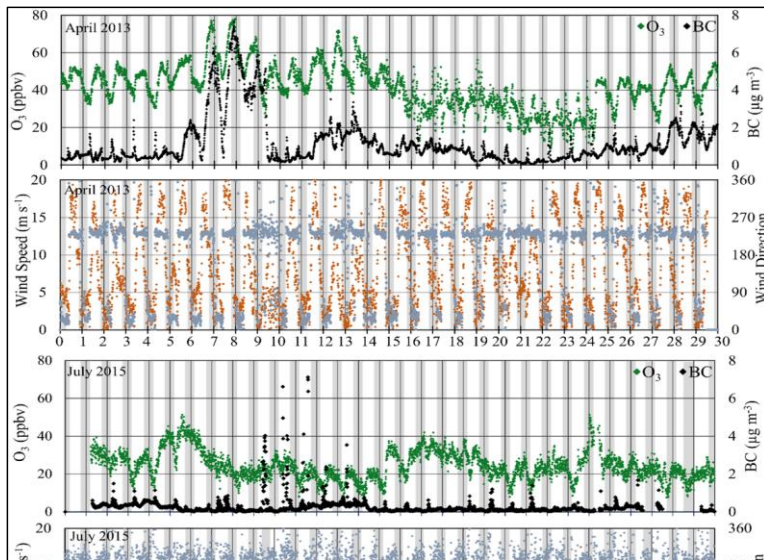
970

975

980

985

990



995

1000

1005

1010

[NEW] Table 1. Comparison of BC and O₃ concentrations between high elevation Himalayan site NCO-P CNR and JSM_1.

Sites	Altitude (m)	Co-ordinates	Season	BC ($\mu\text{g m}^{-3}$)	O ₃ (ppb)
NCO-P Nepal Climate Observatory Pyramid (Bonasoni et al., 2010)	5079	27.95° N, 86.81° E	Pre-monsoon	0.317 (± 0.34)	60.9 (± 8.4)
			Monsoon	0.049 (± 0.06)	38.9 (± 9)
			Post-monsoon	0.135 (± 0.08)	46.3 (± 5.0)
JSM_1(Jomsom) Kali Gandaki Valley	2800	28.87° N, 83.73° E	Pre-monsoon	0.891 (± 0.45)	39.5 (± 8.23)
			Monsoon	0.207 (± 0.24)	25.1 (± 6.48)
			Post-monsoon	0.714 (± 0.42)	31.4 (± 4.5)

1015

1020

1025

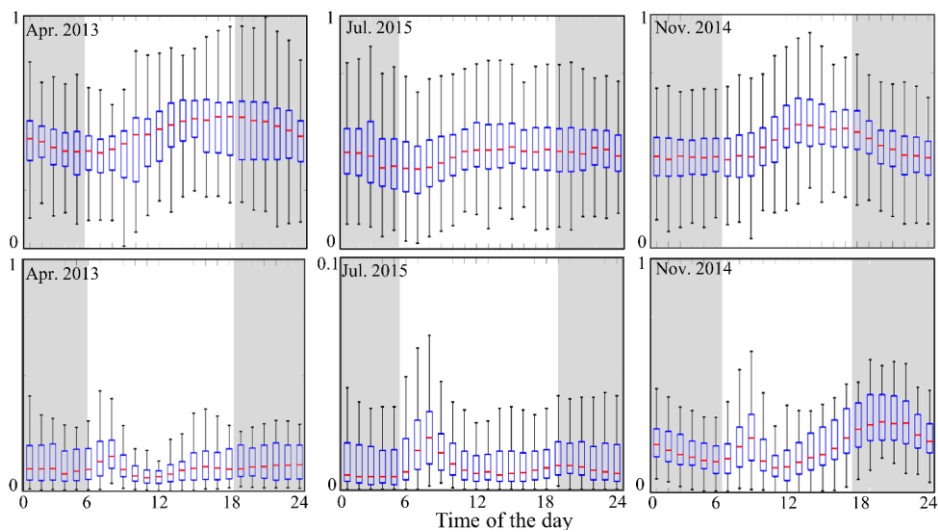


Figure 4-5 Box and whisker plots depicting the 90th, 75th, 50th, 25th, and 10th percentiles for normalized diel variability in O₃ (upper panels) and BC (lower panels) at JSM_STA during April 2013 (pre-monsoon), July 2015 (monsoon), and November 2014 (post-monsoon). Scale for July 2015 is from 0 to 0.1.

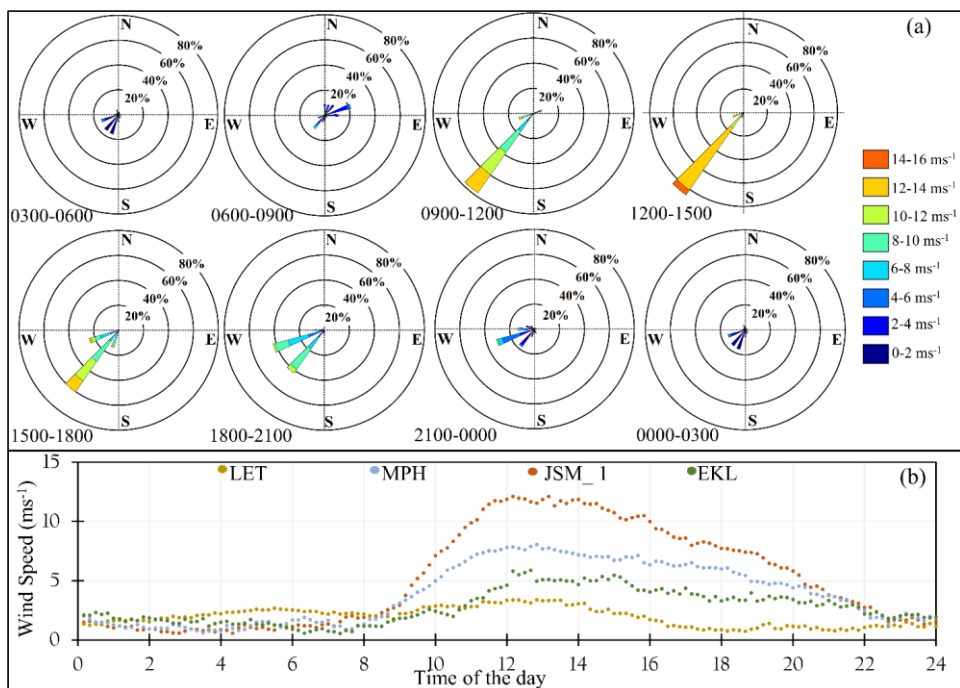
1030

1035

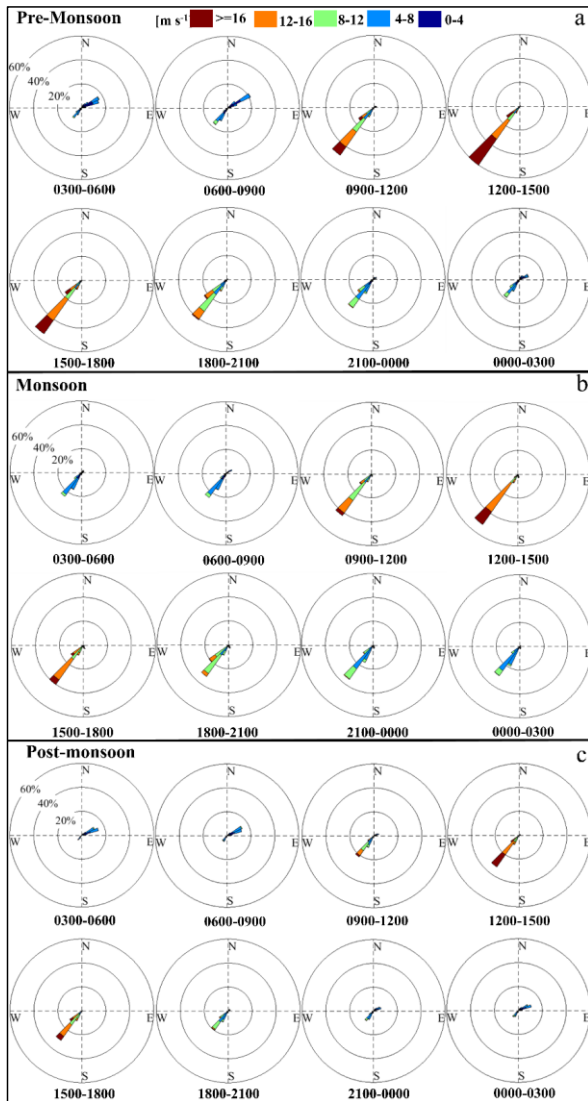
1040

1045

1050



MOVED TO SUPPLEMENTARY FIGURES Figure 5. (a) Wind rose for data from May 8 to 14, 2015 binned into 3-hour increments depicting diurnal evolution in wind speed and direction at JSM_2. (b) Corresponding diurnal variability in wind speed based on average values over the same period at LET, MPH, JSM_2 and EKL.



NEW Figure 6. (a) Wind rose for each season binned into 3-hour increments depicting diurnal evolution in wind speed and direction at JSM_2.

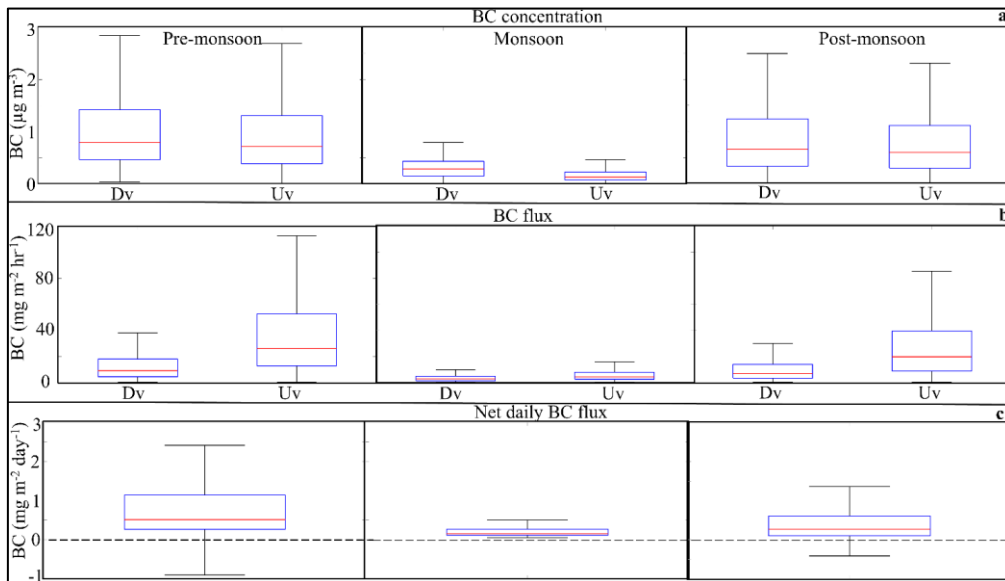
1090

1095

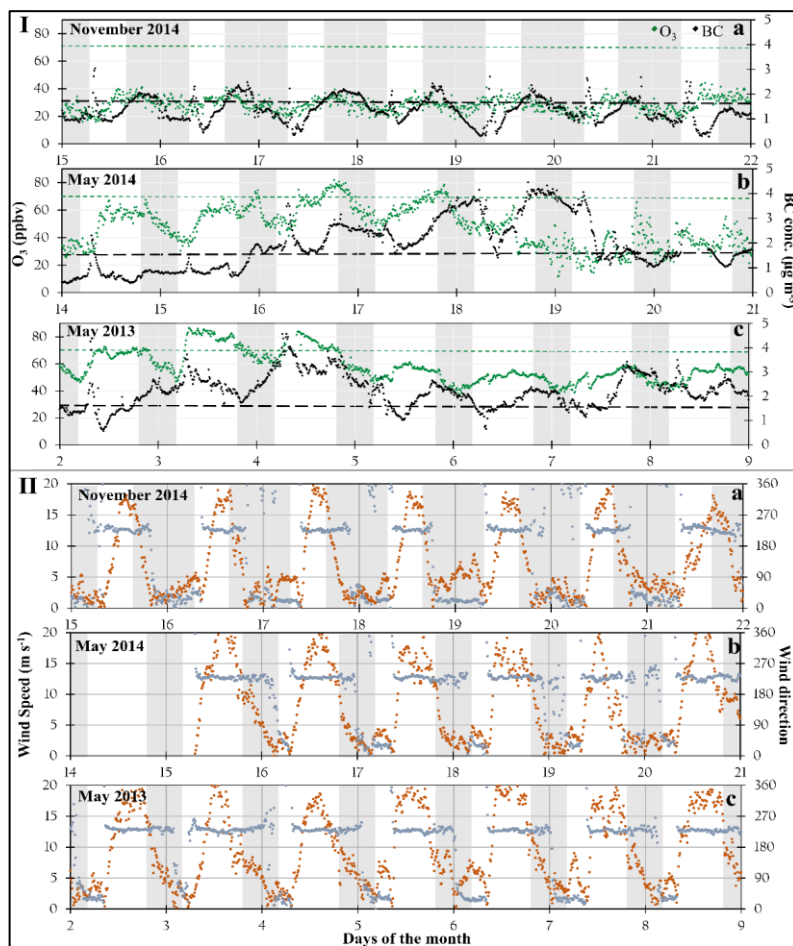
1100

1105

1110



NEW Figure 7. (a) BC concentration distribution with down-valley (Dv) and up-valley (Uv) flows in Jomsom, (b) calculated Dv and Uv flux for each season, (c) Net daily flux per season. The dotted line is panel c marks $0 \text{ mg m}^{-2} \text{ day}^{-1}$.



UPDATED Figure 88. (I) Examples of extended periods with relatively high BC and O₃ concentrations at JSM_STA during November 2014 (Pattern A) and May 2014 (Pattern B) and May 2013 (Pattern C). The solid black and green lines depict two-year averages for BC and O₃, respectively. (II) Corresponding wind direction and wind speed during the high BC and O₃ episodes.

1115

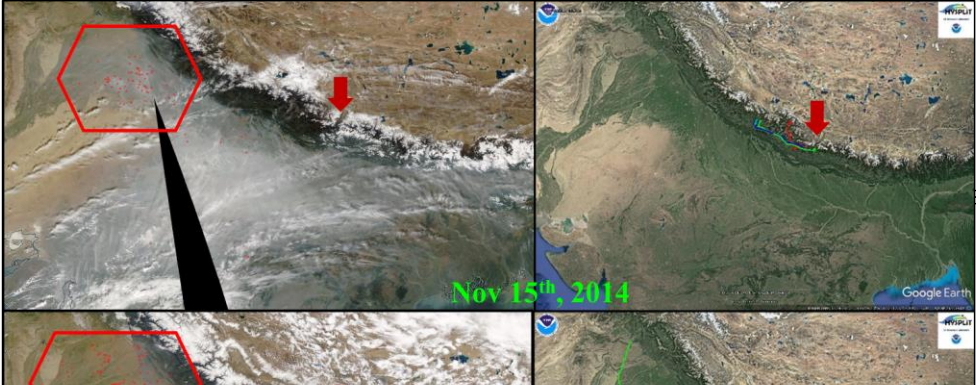
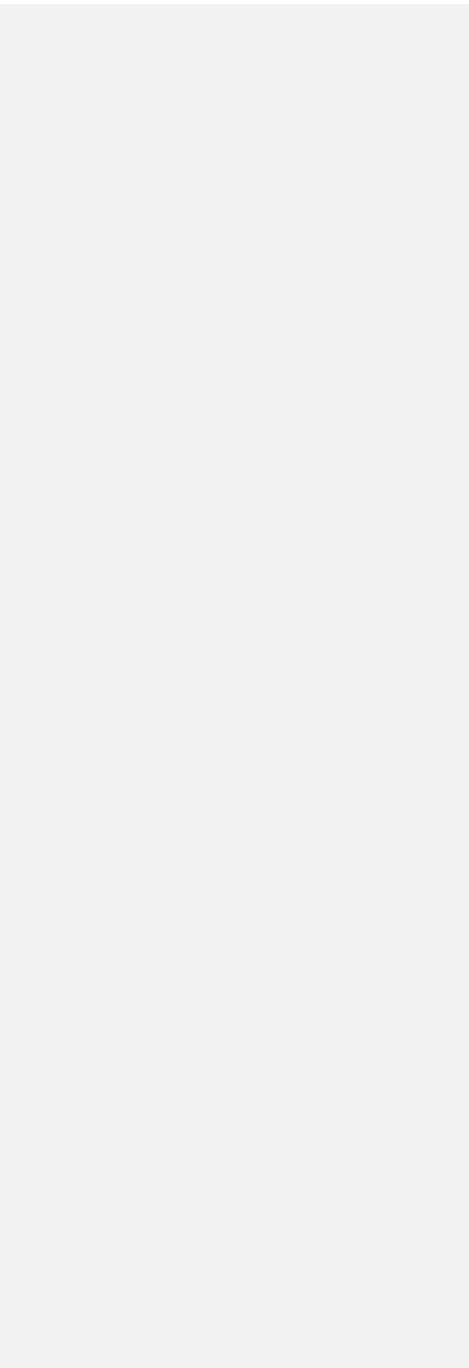
1120

1125

1130

1135

1140



1145

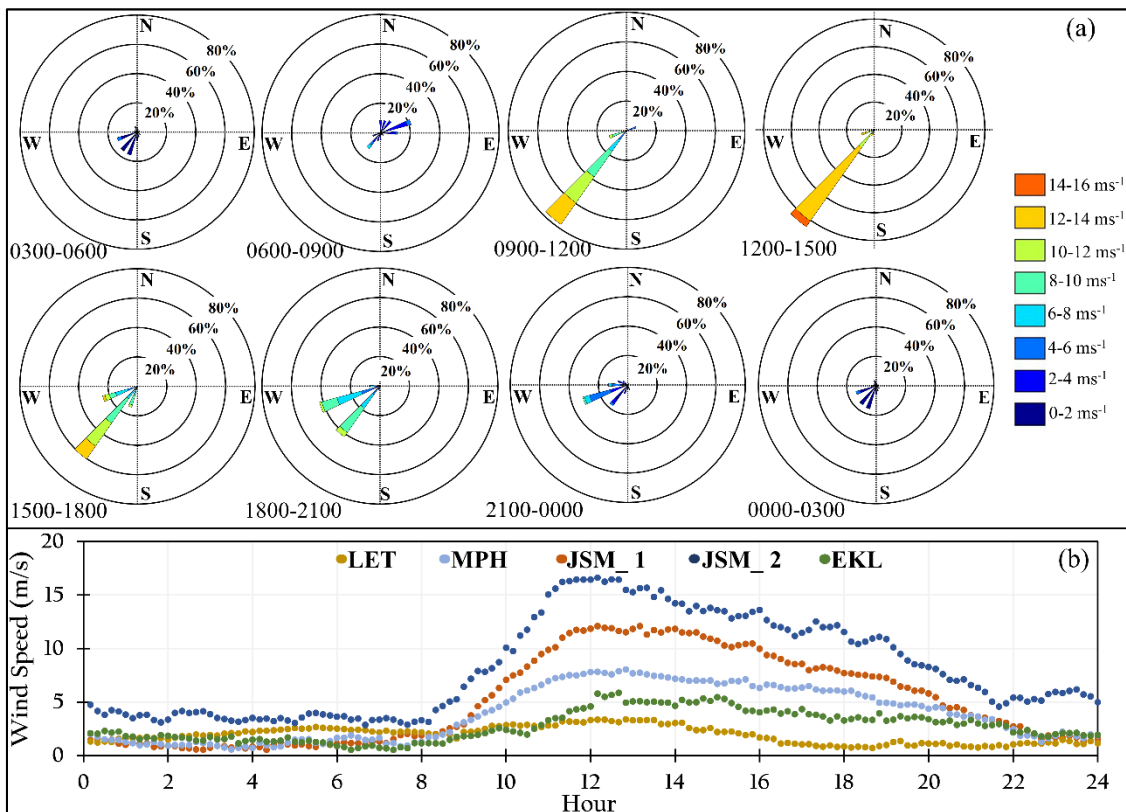
1150

1155

1160

NEW Supplementary Table 1. Data timeline for JSM_2 AWS, BC and O₃ measurements in Jomsom. Green indicates complete data, blue is with few data points missing, yellow is more than 15 days data, orange is less than 15 days and blank is no data.

Year	2013												2014												2015											
Month	J	F	M	A	M	J	J	A	S	O	N	D	J	F	M	A	M	J	J	A	S	O	N	D	J	F	M	A	M	J	J	A				
AWS-D	Green	Green	Green	Green	Green	Green	Green	Green	Green	Green	Green	Green	Green	Green	Green	Green	Green	Green	Green	Green	Green	Green	Green	Green	Green	Green	Green	Green	Green	Green	Green	Green				
BC	Yellow	Green	Green	Green	Green	Green	Green	Green	Green	Green	Green	Green	Green	Green	Green	Green	Green	Green	Green	Green	Green	Green	Green	Green	Green	Green	Green	Green	Green	Green	Green	Green				
O ₃	Yellow	Yellow	Green	Green	Green	Green	Green	Green	Green	Green	Green	Green	Green	Green	Green	Green	Green	Green	Green	Green	Green	Green	Green	Green	Green	Green	Green	Green	Green	Green	Green	Green				



MOVED FROM THE MANUSCRIPT Supplementary Figure 1 (a) Wind rose for data from May 8 to 14, 2015 binned into 3-hour increments depicting diurnal evolution in wind speed and direction at JSM_1. (b) Corresponding diurnal variability in wind speed based on average values over the same period at LET, MPH, JSM_1 and EKL.

NEW Supplementary Table 2 Mean, median and percentage distribution for BC concentration and flux for up-valley and down-valley flows. Net daily flux for each season and its percentage distribution.

Season	Variable	Northeasterly (down-valley)			Southwesterly (up-valley)			Difference		
		Mean	Median	75th Percentile	Mean	Median	75th Percentile	Mean	Median	75th percentile
Pre-monsoon	BC concentration	1.060	0.793	0.464	1.420	0.980	1.307	0.080	0.080	0.113
	BC flux	14.088	9.134	4.573	18.160	38.030	12.756	-23.942	-17.043	-8.183
	Net flux*	0.750	0.510	0.260	1.143					-34.652
Monsoon	BC concentration	0.375	0.280	0.150	0.430	0.179	0.227	0.196	0.153	0.203
	BC flux	3.980	2.636	1.182	4.555	5.984	2.240	-2.004	-1.427	-3.037
	Net flux*	0.220	0.147	0.108	0.271					
Post-monsoon	BC concentration	0.800	0.653	0.327	1.237	0.730	1.110	0.070	0.053	0.127
	BC flux	10.436	6.700	3.184	13.874	27.020	2.240	-16.584	-12.830	0.944
	Net flux*	0.372	0.275	0.980	0.604					

NEW Supplementary Table 3. List of enhanced BC episodes observed at JSM_STA and the concurring regional sources from MODIS (* Data is from January-July)

60

65

70

75

80

2013 (90th Percentile = 1.53)			
MONTH	EPISODE LENGTH	EPISODE TYPE	SOURCE LOCATION
Jan	6th-15th	C	Haze
	28th-31st	C	fire in the Punjab region of Pakistan
Feb	Jan (contd.)- Feb 2nd	C	Haze
Mar	1st-3rd	A	Haze along with fires west of Nepal in northern India
	6th-9th	A	fire in the Punjab region of Pakistan
	11th-13th	B	fire in the Punjab region of Pakistan
	18th-27th	B	fire in the Punjab region of Pakistan and scattered fire in Northern India, west of Nepal
Apr	6th-10th	B	fire in the Punjab region of Pakistan and in central and western Nepal
	12th-14th	B	fire in the Punjab region of Pakistan and fire in central Nepal
	27th-30th	A	fire in the Punjab region of Pakistan and in Northern India-west of Nepal; Haze
May	3rd-11th	B	fire in the punjab region of India (over 100 events) and in Pakistan
Oct	28th-30th	A	fire in the punjab region of India and Pakistan and Haze
Nov	1st-5th	A	fire in the punjab region of India and Haze
	23rd-30th	A	Haze
Dec	17th-24th	C	Haze
2014 (90th Percentile=1.60)			
MONTH	EPISODE LENGTH	EPISODE TYPE	SOURCE LOCATION
Jan	13th-15th	A	Cloud cover
Feb	Jan31st-Feb 1st	A	high cloud cover
Mar	14th-16th	A	fire in Punjab region of Pakistan
Apr	5th-8th	B	fire in central and western Nepal and Haze
	10th-30th	C	fire events in Punjab, India and Pakistan
May	Apr 10th-May 1st	C	fire in western Nepal, central India and Punjab, Pakistan
	8th-13th	B	fire in western Nepal and over 150 fire events in the Punjab region of India and Pakistan
	17th-23rd	C	fire in India-west of Nepal- and over 100 fire events in the Punjab region of India and Pakistan
Jun	5th-8th	B	fire in India-west of Nepal (Uttarakhand-India)
	10th-17th	B	fire in the foothills of the Himalaya (western Nepal and northern India-west of Nepal)
Nov	15th-30th	A	Haze and fire events in India
Dec	Nov 15th-Dec 8th	A	Haze and a few fire events in Punjab, Pakistan
2015 (90th Percentile=1.47)*			
MONTH	EPISODE LENGTH	EPISODE TYPE	SOURCE LOCATION
Jan	15th-17th	A	Cloudy/indeterminant
	21st-25th	A	Cloudy/indeterminant
Feb	21st-26th	A	Cloudy/indeterminant
May	6th-9th	A	Extensive butning (over 200 fire events) in Punjab region of Pakistan and India
	18th-26th	A	fire events in the western region of Nepal and Northern India- southwest of Nepal
	29th-31st	B	Fire in northern India-west of Nepal (Uttarakhand) and western Nepal
Jun	6th-12th	B	Fire in northern India-west of Nepal (Uttarakhand) and western Nepal